

## Supporting Information

### A machine learning approach for dynamical modelling of Al distributions in zeolites via $^{23}\text{Na}/^{27}\text{Al}$ solid-state NMR

Chen Lei,<sup>a</sup> Carlos Bornes,<sup>a</sup> Oscar Bengtsson,<sup>b</sup> Andreas Erlebach<sup>a</sup>, Ben Slater,<sup>b</sup> Lukas Grajciar<sup>a</sup> and Christopher J. Heard\*<sup>a</sup>

<sup>a</sup> Department of Physical and Macromolecular Chemistry, Faculty of Science, Charles University in Prague, 12483, Czech Republic. E-mail: heardc@natur.cuni.cz  
<sup>b</sup> Department of Chemistry, University College London, 20 Gordon Street, London WC1H 0AJ, UK.

# 1 Workflow Scheme

1. Configuration generation with NNP
2. Filtering of low energy configurations ( $< 20 \text{ kJ mol}^{-1}$ )
3. NNP MD simulations (NVT, 350 K, 1 ns)
4. Collection of snapshots along MD trajectory (100 points)
5. DFT NMR calculations (CASTEP) for  $^{23}\text{Na}$  and  $^{27}\text{Al}$  nuclei
6. Averaging of EFG ( $[G_i]$ ) and shielding ( $[\sigma_i]$ ) tensors
7. Extraction of  $\delta_{\text{iso}}$ ,  $C_Q$ ,  $\eta$  from  $\overline{[G]}$  and  $\overline{[\sigma]}$

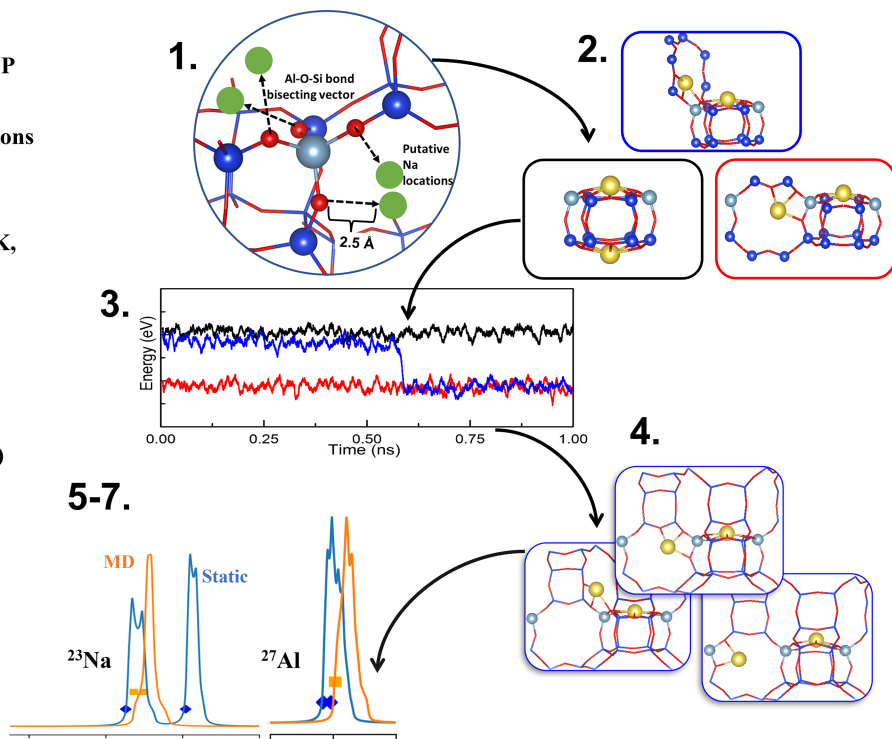


Fig. S1 Schematic of the computational workflow for the calculation of dynamically averaged  $^{27}\text{Al}$  and  $^{23}\text{Na}$  spectra for relevant, low-energy configurations.

## 2 Na configurations

### 2.1 CHA35

The static Na configurations of CHA35 are shown in Fig.S2. The  $\text{Na}^+$  tends to bind preferentially to the positions near Al, and 6MR(1Al) (SII) is the lowest energy case (a).

There are several energetically uncompetitive local minima for 6MR(0Al) environments. Comparison between them reveals that the Na cation prefers to be located at the 6-ring face connected (within one double six-ring) to an Al site (Figure S2(d)).

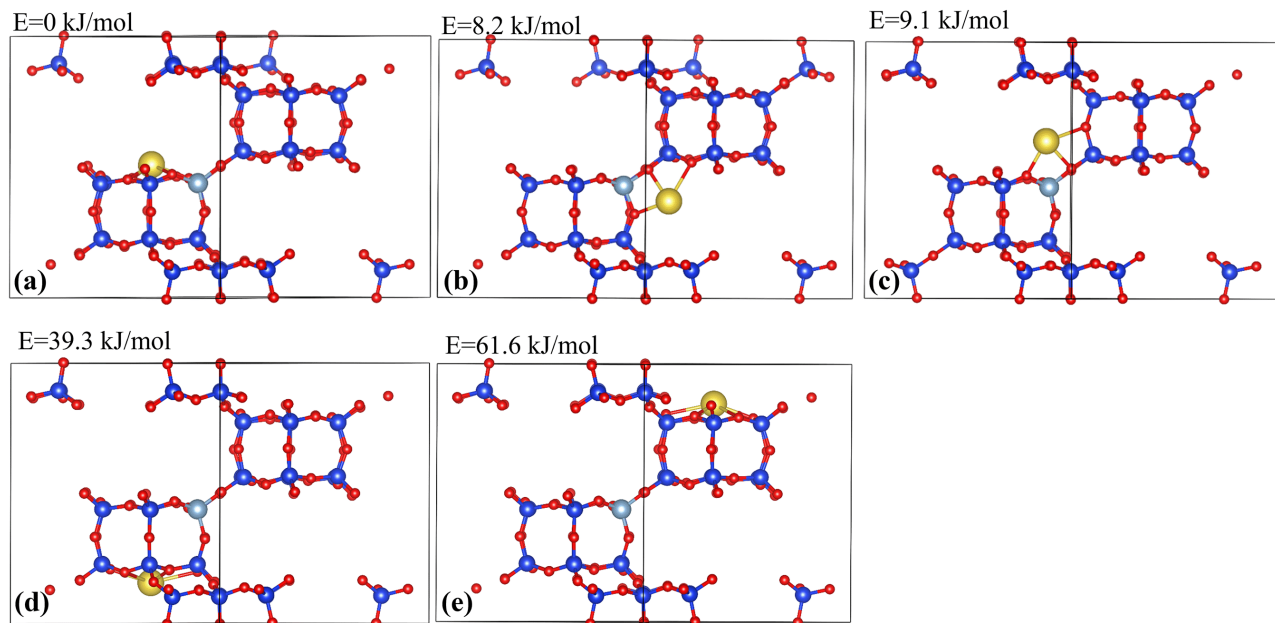
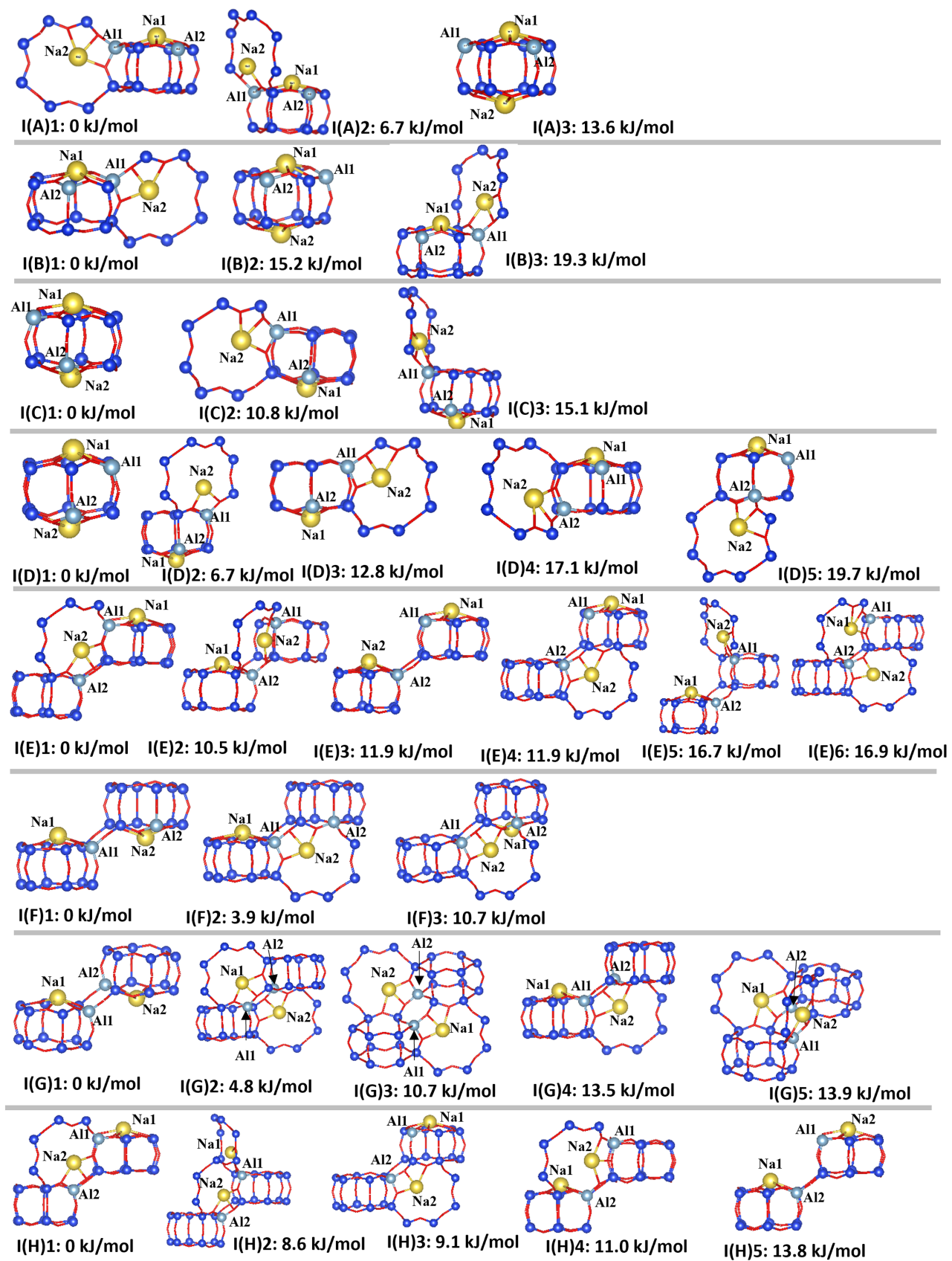
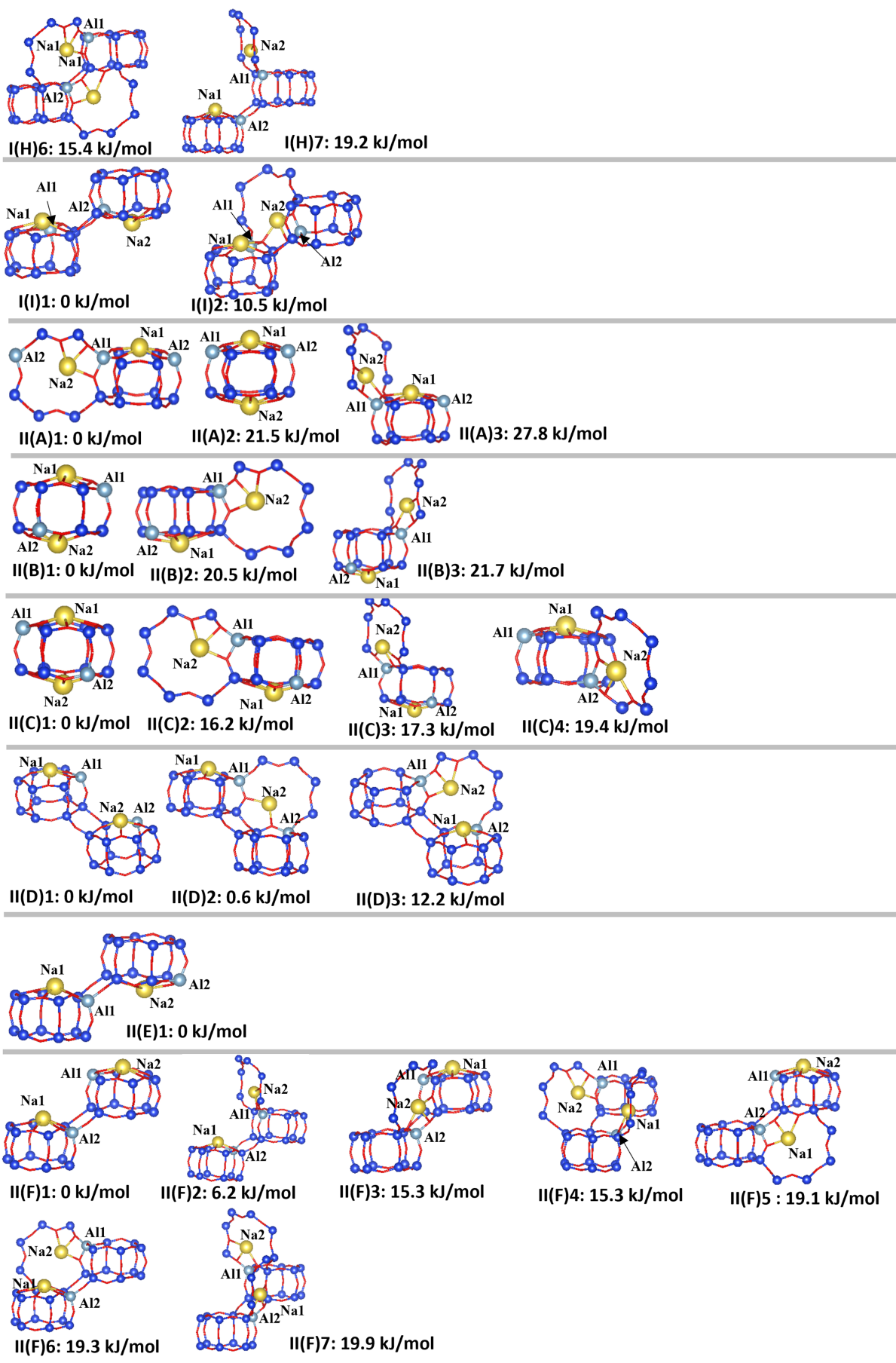
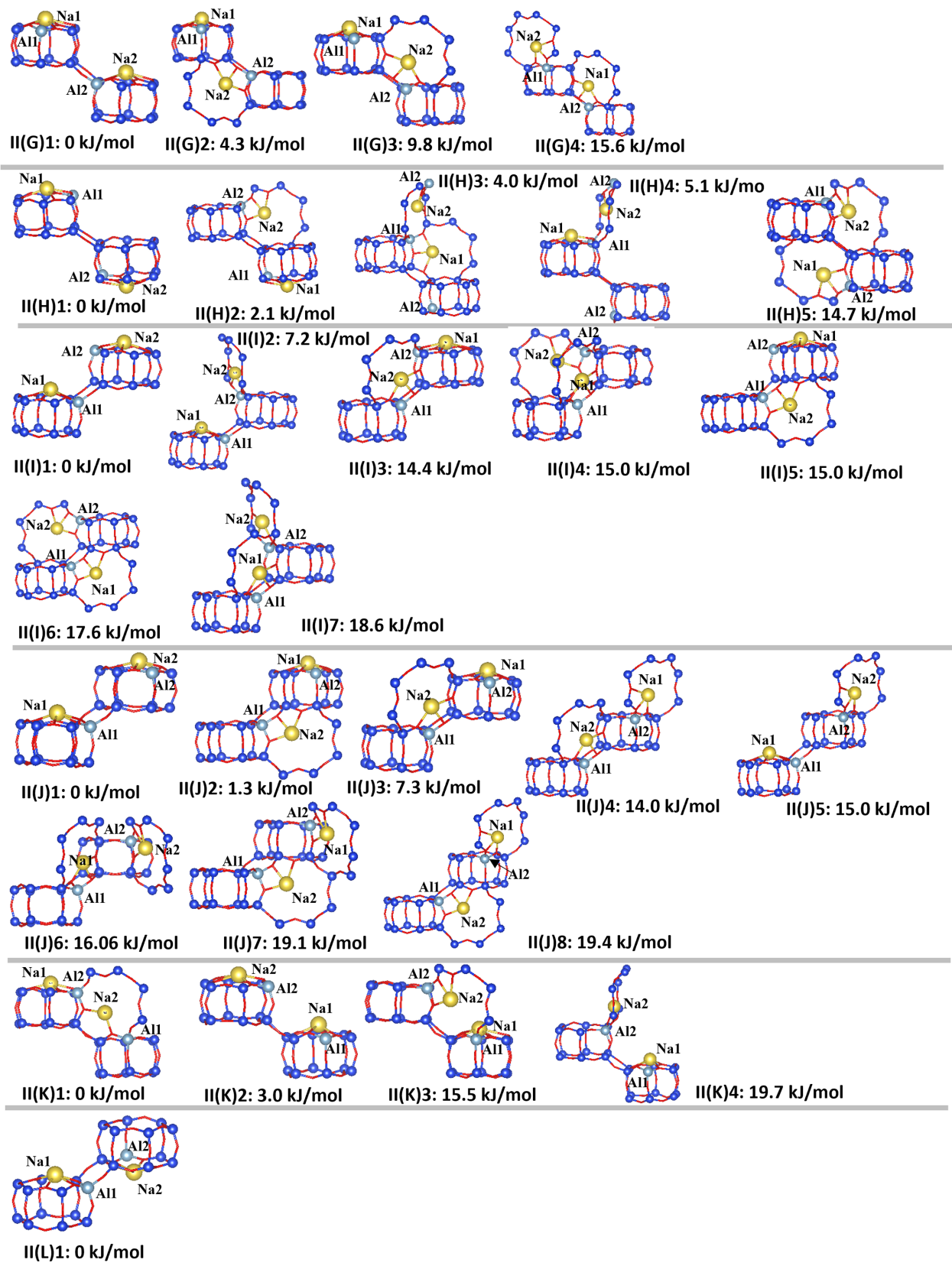


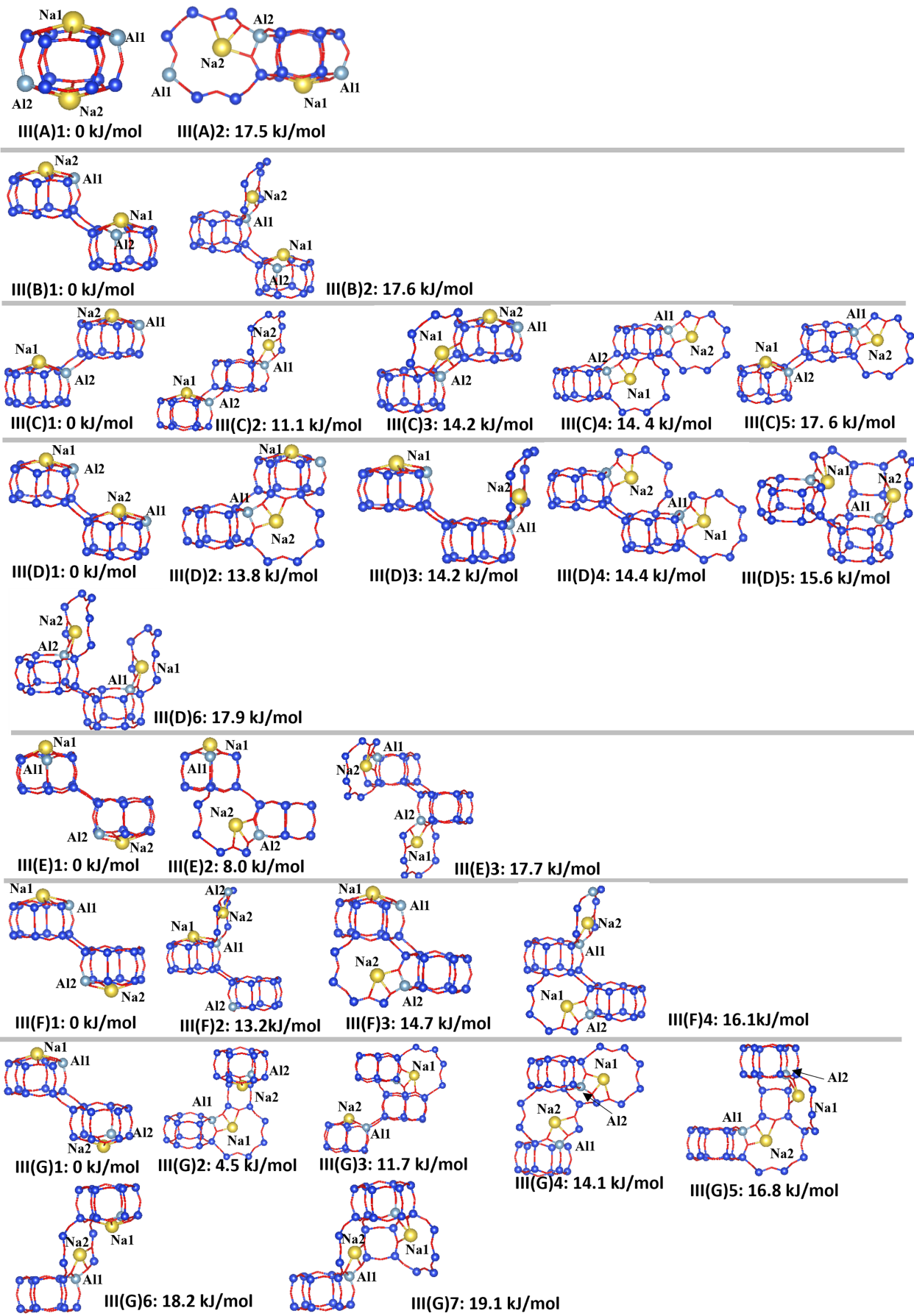
Fig. S2 The structures of CHA35 of different  $\text{Na}^+$  configurations. a) the lowest energy case with Na on the 6MR window, b) and c) Na on the 8MR(1Al) window SIII and SIII' sites, d) and e) Na on the all-Si 6MR windows sharing the same  $d6r$  with Al site and on another all-Si  $d6r$ , respectively. The energy report here is from DFT static calculations.

## 2.2 CHA17









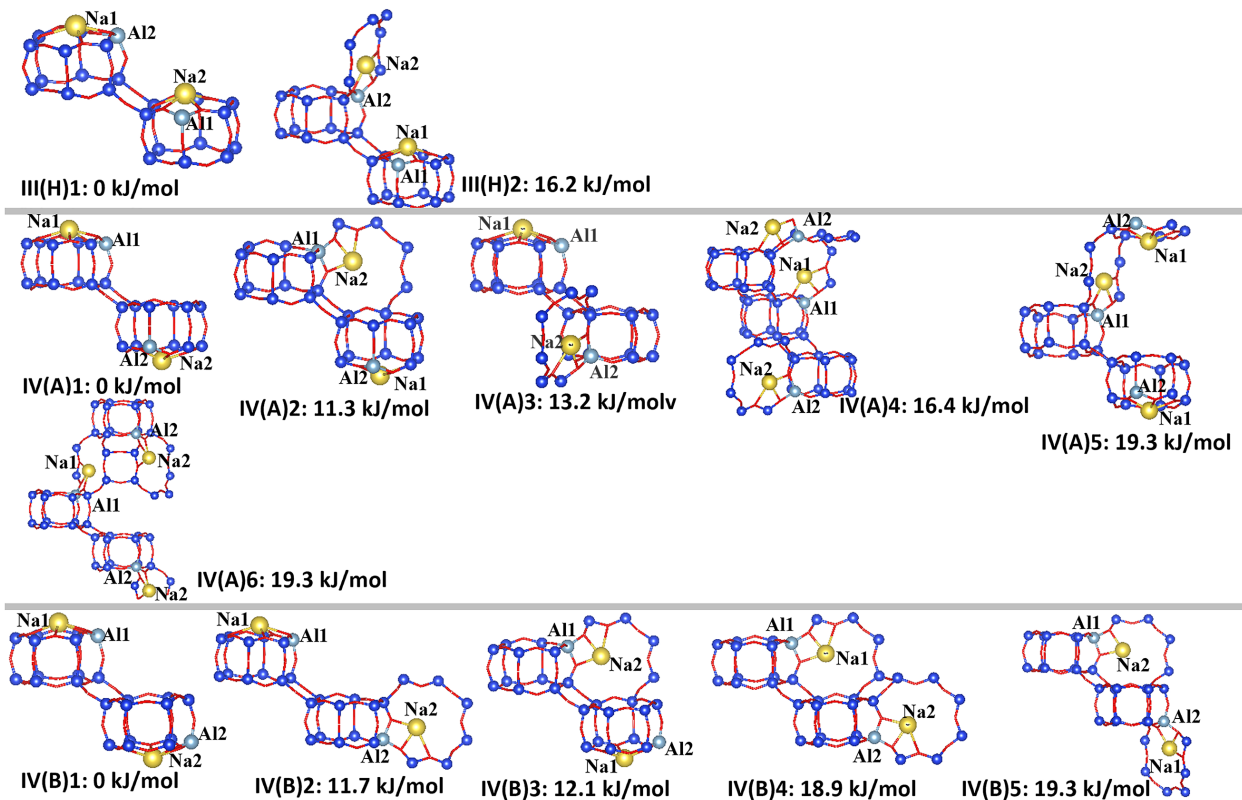


Fig. S3 The local structures of all the CHA(17) models to do the NMR calculations. The cases with molecular dynamics calculations are: I(A)1, I(A)3, I(C)1, I(C)2, I(C)3, I(E)1, I(E)3, I(F)1, I(F)2, I(G)1, I(G)3, II(A)1, II(A)2, II(A)3, III(A)1, III(A)2, III(E)2, III(F)1, III(F)3, IV(A)1 and IV(A)3. The energy report here is from DFT static calculations.

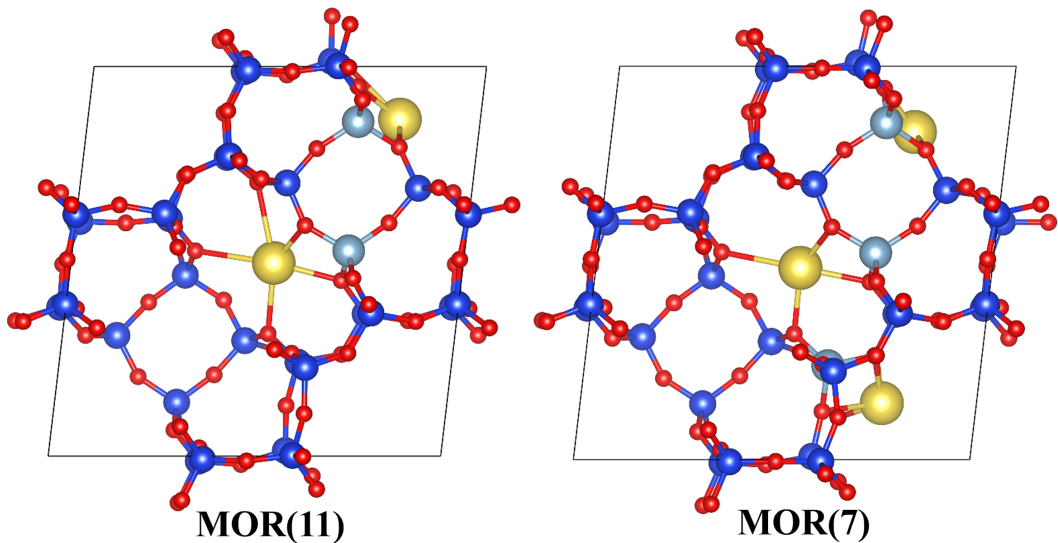


Fig. S4 The models of MOR with Si/Al 11 and 7. In MOR(11)(left), two Al substitutions are T3 and T4 sites. In MOR(7)(right), three Al substitution are T1, T3 and T4 sites.

### 3 DFT dataset for NNP training

Table S1 Number of T-sites ( $N_t$ ), aluminum/sodium atoms ( $N_{\text{Al}}$ ,  $N_{\text{Na}}$ ) and water molecules ( $N_w$ ), database index (ID) of the hypothetical zeolite database published in Ref.<sup>1</sup>, and framework density (FD in  $N_t$  per nm<sup>3</sup>) of the initial structures constructed for database creation using existing zeolite topologies (CHA, SOD, MVY), hypothetical frameworks (HYP) and a silica bilayer (BL).

Topology	ID	FD	$N_t$	$N_{\text{Al}} = N_{\text{Na}}$	$N_w$			
CHA	-	14.9	12	1 3 6	0	2	6	12
SOD	-	17.8	12	1 3 6	0	2	4	8
MVY	-	20.5	24	2 6 11	0	2	4	6
HYP1	17883	23.2	14	1 4 6	0	1	2	3
HYP2	2251	19.5	16	1 3 5	0	2	4	8
HYP3	17089	20.9	32	1 7 14	0	2	5	10
HYP4	46458	21.5	28	1 5 10	0	1	2	4
HYP5	4552	20.1	32	1 5 10	0	1	3	7
HYP6	9330	19.2	16	1 3 6	0	2	5	10
HYP7	72920	15.8	24	1 5 9	0	5	15	25
BL	-	9.7	24	3 6 9	0	10	25	55

Table S2 Chemical composition of sodium aluminosilicate polymorphs used for DFT dataset creation.

Polymorph	$N_{\text{Si}}$	$N_{\text{O}}$	$N_{\text{H}}$	$N_{\text{Na}}$	$N_{\text{Al}}$
Analcime <sup>a</sup>	32	112	32	16	16
Grumantite <sup>a</sup>	8	24	12	4	0
$\text{Na}_5(\text{Al}(\text{OH})_6)(\text{OH})_2$ <sup>b</sup>	0	32	32	20	4
$\text{NaOH}$ <sup>b</sup>	0	2	2	2	0
Natrolite <sup>a</sup>	24	96	32	16	16
Ussingite <sup>a</sup>	6	18	2	4	2
Carnegieite <sup>a</sup>	4	16	0	4	4
Diaoyudaoite <sup>a</sup>	0	34	0	2	22
Jadeite <sup>a</sup>	8	24	0	4	4
$\text{Na}_2\text{O}$ <sup>a</sup>	0	4	0	8	0
Natrosilite <sup>a</sup>	8	20	0	8	0
Nepheline <sup>a</sup>	8	32	0	8	8

<sup>a</sup>available under: <https://rruff.geo.arizona.edu/AMS/amcsd.php>; <sup>b</sup>available under: <https://www.crystallography.net/cod/>

## 4 Referencing for the $^{23}\text{Na}$ chemical shift

There are two ways to produce the calculated chemical shift ( $\delta_{iso}$ ) from DFT calculated chemical shielding ( $\sigma$ ) to compare with the experimental spectra: a) using the exact experimental reference compound  $\sigma$  as the reference,  $\delta_{cal} = \sigma_{cal} - \sigma_{ref}$ ; b) referencing from a series of compounds to obtain a linear regression that cancels errors better,  $\delta_{cal} = a\sigma_{cal} + b$ .<sup>2</sup> The second strategy was adopted in this work.

Single point calculations of local minimum geometries of a set of six relevant reference systems were made with the PBEsol xc-functional within the CASTEP software. It can be seen in Figure S5, that the set of reference compounds yields a good linear fit, with a gradient of 0.86, and that the choice of cutoff energy for CASTEP calculations leads to a systematic offset of around 3 ppm in  $\sigma_{cal}$ . Thus the resulting calibration between  $\sigma_{cal}$  and  $\delta_{cal}$  is independent of energy cutoff, and we subsequently choose 700 eV for production calculations.

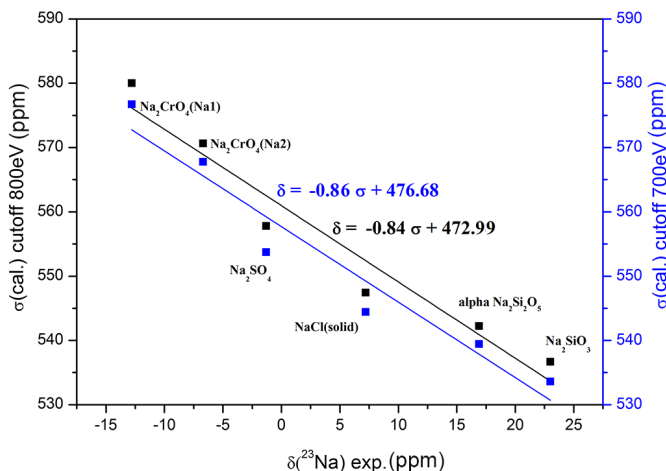


Fig. S5 A linear regression between the experimental chemical shift  $\delta_{iso}$  and calculated chemical shielding  $\sigma$ . The black one is based on the result of the 800 eV cutoff and the blue one is 700 eV cutoff.

## 5 $^{23}\text{Na}$ NMR LASSO regression in zeolites

The least absolute shrinkage and selection operator (LASSO) regression was applied to select the most relevant structural features for linear correlation of DFT calculated  $^{23}\text{Na}$  chemical shielding  $\sigma$  and the atomic environments related to Na atoms. LASSO regression minimizes an objective function  $L$  with the error sum of squares over  $n$  samples between target values  $\sigma_{i,DFT}$  and a linear model  $\sum_{j=1}^p c_j \cdot x_{ij}$  with  $p$  coefficients  $c_j$  and the structural features  $x_{ij}$ :

$$L = \frac{1}{n} \sum_{i=1}^n (\sigma_{i,DFT} - \sum_{j=1}^p c_j \cdot x_{ij})^2 + \lambda (\sum_{j=1}^p |c_j|).$$

The L1 regularization term  $\lambda (\sum_{j=1}^p |c_j|)$  with hyperparameter  $\lambda$  acts as penalization of  $c_j$  allowing them to go to zero during minimization of  $L$  and, therefore, feature selection. All LASSO regressions used regularization parameters  $\lambda \in [10^0, 10^{-3}]$  and 80% of DFT calculations for training and the remaining data points as test sets.

The LASSO regression used twenty-five structural features (see TableS3) and about 6232 DFT points of CHA(17) to test the importance of local descriptors around Na and the local descriptors (framework) influenced by Na such as Al-O distance and Al-O-Si angles. Notably, it is investigated that the definition of the coordination sphere of Na can lead to much difference in chemical shift prediction with structural features in sodium silicate compounds(up to 10 ppm difference).<sup>3</sup> Here we tested different cutoffs to define the coordination spheres in CHA zeolite. It is shown the influence of Na-Si and Na-Al cutoffs are negligible due to their small contribution to  $^{23}\text{Na}$   $\sigma$  (Table S5), but that of the Na-O cutoff is significant by comparison of 3.0 and 3.5 Å. The correlation with calculating Na-O descriptors in 3.0 Å coverestimated the cases with chemical shielding in two ends (Figure S6). The features were calculated with the O coordination sphere of Na in 3.5 Å, which agrees with the definition in the work by Koller<sup>4</sup> (3.4 Å).

Table S3 Local features considered in LASSO regression including average distances d and angles  $\alpha$  as well as the corresponding difference ( $\Delta d$ ,  $\Delta \alpha$ ) between minimum and maximum values (spread) of the features.

Local features of Na	Cutoff of the neighbor atoms (Å)
$CN_{Na-O}$	Coordination numbers of the Na-O
$CN_{Na-O(Al)}$	Coordination numbers of the Na-O connect to Al
$CN_{Na-Si}$	Coordination numbers of the Na-Si
$CN_{Na-Al}$	Coordination numbers of the Na-Al
$d_{Na-O}$	Mean Na-O distance
$d_{Na-O(Al)}$	Mean Na-O distance with O connect to Al
$d_{Na-Si}$	Mean Na-Si distance
$d_{Na-Al}$	Mean Na-Al distance
$\alpha_{O-Na-O}$	Mean O-Na-O angle
$\alpha_{Al-Na-Al}$	Mean Al-Na-Al angle
$\Delta d_{Na-O}$	Spread of Na-O distances
$\Delta d_{Na-Si}$	Spread of Na-Si distances
$\Delta d_{Na-Al}$	Spread of Na-Al distances
$\Delta \alpha_{O-Na-O}$	Spread of O-Na-O angles
$d_{Na-O}^{min}$	Minimum Na-O distance with O connect to Al
$d_{Na-O(Al)}^{min}$	Minimum Na-O distance
$d_{Na-Si}^{min}$	Minimum Na-Si distance
$d_{Na-Al}^{min}$	Minimum Na-Al distance
Framework features	
$d_{Al-O}$	Mean Al-O distance (Al closest to Na)
$\alpha_{Al-O-Si}$	Mean Al-O-Si angle
$\alpha_{T-O-T}$	Mean T-O-T angle (O neighbor to Na)
$\Delta d_{Al-O}$	Spread of Al-O distances
$\Delta \alpha_{Al-O-Si}$	Spread of Al-O-Si angles
$\alpha_{T-O-T}^{min}$	Minimum T-O-T angle (O neighbor to Na)

It turned out that seven features yield a coefficient of determination  $R^2$  of 0.82 and using additional descriptors provides virtually no improvement (see Figure S6 d). The features  $CN_{Na-O}$ ,  $CN_{Na-Si}$ ,  $d_{Na-O}$ ,  $\alpha_{O-Na-O}$ ,  $d_{Na-O}^{min}$ ,  $d_{Na-Si}^{min}$ , and  $CN_{Na-O(Al)}$  were used for (unregularized) linear regression and yield a coefficient of determination  $R^2$  of 0.88 and MAE of 2.5 ppm. Next, one test dataset with 1521 points of CHA(35) and CHA(11) and one dataset with 1005 points of MOR(11) and MOR(7) datasets was used to test the regression generalization of the equation4 (Fig.S6 f). This is described in the Results part.

Following the previous empirical works which connected the  $^{23}\text{Na}$   $\delta_{iso}$  with  $d_{Na-O}^{min}$  or  $d_{Na-O}$ , the one descriptor regressions were tested on our dataset.(Figure S6) The results show that one descriptor is not enough to predict  $^{23}\text{Na}$   $\delta_{iso}$  in the zeolite CHA system(more than 6 ppm errors from DFT calculations), although the  $d_{Na-O}^{min}$  show better correlation. The tendency of  $d_{Na-O}^{min}$  correlation better than the  $d_{Na-O}$  agrees with the results of Steinadler et al in the compounds with pure oxygen environment Na,<sup>5</sup> but the correlation in zeolite system is worse(0.43 R<sup>2</sup> and 6.3 ppm MAE). Then a correlation was done with two most important factors from LASSO,  $\alpha_{O-Na-O}$  and  $d_{Na-O}^{min}$ , which shows 0.653 R<sup>2</sup> and 4.52 ppm MAE on the CHA(17) dataset(Figure S6c). Although it still failed to describe many points, the tendency is clear. Namely, the oxygen environment around Na affects the isotropic chemical shift mainly in zeolites, and the Al environment ( $d_{Na-O}^{min}$  and  $CN_{Na-O(Al)}$ ) is important to describe some special Na positions.

For the calculation of  $^{27}\text{Al}$  solid state NMR chemical shieldings, we used the LASSO regression formula that was previously obtained for high silica Al-CHA, from ref<sup>6</sup>. In order to test its viability in Na-CHA, we performed a correlation between DFT calculations of chemical shift and the LASSO predictions for various Na-zeolite models, namely CHA(35), CHA(17), CHA(11), MOR(11) and MOR(7). This stern test of the generalization of the original regression is plotted in Figure S7. We observe that over the full dataset, the correlation remains good, with a coefficient of 0.84, and an MAE value of 1.2 ppm. The errors are highest for the CHA(11) and MOR(7) models, as expected, owing to their low Si/Al ratio. Nevertheless, the correlation remains good, with MAEs below 1.7 ppm for all tested datasets.

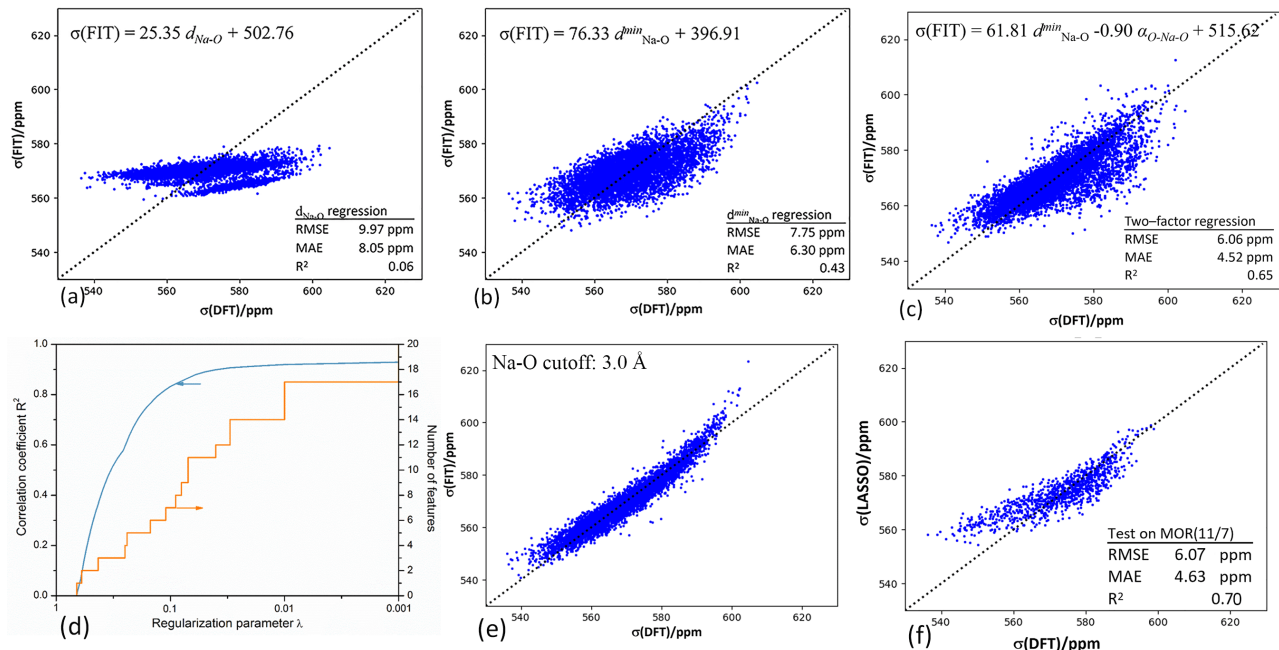
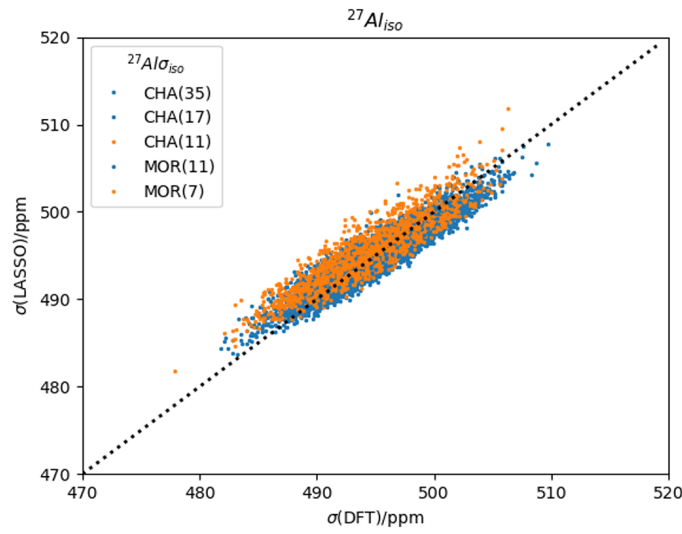


Fig. S6 The one descriptor regression with  $d_{Na-O}$  and  $d_{Na-O}^{min}$  (a) and (b). The two descriptors regression with the two important descriptors selected from LASSO,  $d_{Na-O}^{min}$  and  $\alpha_{O-Na-O}$  (c). Coefficient of determination  $R^2$  of the employed test set and the number of structural features with non-zero coefficients as a function of the LASSO regularization parameter  $\lambda$  (d). A test of the LASSO regression model against the training set of chemical shielding of CHA(17) configurations with calculating descriptors about Na-O in 3.0 Å (e). The test of the seven-factor equation 4 on the MOR dataset (f).



Dataset	R <sup>2</sup>	MAE(ppm)	RMSE(ppm)
full dataset	0.84	1.25	1.57
CHA35	0.89	1.01	1.23
CHA17	0.86	1.16	1.42
<b>CHA11</b>	<b>0.78</b>	<b>1.64</b>	<b>2.02</b>
MOR11	0.87	1.06	1.35
<b>MOR7</b>	<b>0.69</b>	<b>1.66</b>	<b>2.15</b>

Fig. S7 The LASSO prediction of  $^{27}\text{Al}$   $\sigma$  with the formula from our previous work.<sup>6</sup>

Table S4 The geometric descriptors and their contribution to the  $^{23}\text{Na}$  NMR  $\sigma$  parameters for static NMR calculation in CHA(17). The cases discussed in the text are in bold.

CHA(17)	Geometrical descriptors							Contribution to the $^{23}\text{Na}$ sigma (ppm)						
	CN <sub>Na-O</sub>	d <sub>Na-O</sub> (Å)	CN <sub>Na-Si</sub>	$\alpha_{O-Na-O}$ (°)	d <sub>Na-O</sub> <sup>min</sup> (Å)	d <sub>Na-Si</sub> <sup>min</sup> (Å)	CN <sub>Na-O(AI)</sub>	CN <sub>Na-O</sub>	d <sub>Na-O</sub> (Å)	CN <sub>Na-Si</sub>	$\alpha_{O-Na-O}$ (°)	d <sub>Na-O</sub> <sup>min</sup> (Å)	d <sub>Na-Si</sub> <sup>min</sup> (Å)	CN <sub>Na-O(AI)</sub>
I(A)1	6.00	2.66	5.00	99.05	2.27	3.15	4.00	-35.7	106.9	-3.9	-19.4	104.1	36.4	-8.3
	3.00	2.43	6.00	85.45	2.35	3.10	2.00	-17.9	97.7	-4.7	-16.7	107.5	35.8	-4.1
I(A)3	6.00	2.68	4.00	97.26	2.28	3.16	4.00	-35.7	107.5	-3.2	-19.0	104.4	36.5	-8.3
	6.00	2.61	6.00	98.06	2.37	3.20	0.00	-35.7	104.9	-4.7	-19.2	108.4	37.0	0.0
I(C)1	6.00	2.64	5.00	<b>98.10</b>	2.25	3.18	2.00	-35.7	106.0	-3.9	<b>-19.2</b>	102.8	36.8	-4.1
	6.00	2.66	5.00	97.15	2.29	3.08	2.00	-35.7	106.7	-3.9	<b>-19.0</b>	104.9	35.6	-4.1
I(C)3	6.00	2.65	5.00	98.04	2.28	3.08	2.00	-35.7	106.3	-3.9	-19.2	104.4	35.6	-4.1
	3.00	2.47	7.00	85.05	2.32	3.19	2.00	-17.9	99.0	-5.5	-16.6	106.0	36.9	-4.1
I(E)1	6.00	2.64	5.00	98.74	2.31	3.13	2.00	-35.7	105.9	-3.9	<b>-19.3</b>	105.6	36.2	-4.1
	3.00	2.39	4.00	87.08	2.37	3.01	3.00	-17.9	96.0	-3.2	<b>-17.0</b>	108.7	34.8	-6.2
I(E)3	6.00	2.65	5.00	97.98	2.29	3.11	2.00	-35.7	106.2	-3.9	-19.2	104.7	35.9	-4.1
	6.00	2.67	5.00	96.29	2.27	3.11	2.00	-35.7	107.0	-3.9	-18.8	104.1	35.9	-4.1
I(E)4	6.00	2.65	5.00	97.57	2.27	3.12	2.00	-35.7	106.4	-3.9	-19.1	104.0	36.1	-4.1
	3.00	2.44	7.00	85.60	2.30	3.13	2.00	-17.9	97.9	-5.5	-16.7	105.2	36.1	-4.1
I(F)1	6.00	2.65	5.00	<b>96.99</b>	2.29	3.14	2.00	-35.7	106.2	-3.9	<b>-19.0</b>	104.8	36.3	-4.1
	6.00	2.66	5.00	95.96	2.28	3.07	2.00	-35.7	107.0	-3.9	<b>-18.8</b>	104.5	35.5	-4.1
I(F)2	6.00	2.63	6.00	99.38	2.35	3.14	2.00	-35.7	105.4	-4.7	-19.4	107.7	36.3	-4.1
	3.00	2.41	5.00	85.40	2.32	2.98	3.00	-17.9	96.7	-3.9	-16.7	106.4	34.4	-6.2
I(G)1	6.00	2.65	5.00	97.49	2.27	3.14	2.00	-35.7	106.3	-3.9	-19.1	103.8	36.3	-4.1
	6.00	2.65	5.00	97.59	2.27	3.14	2.00	-35.7	106.2	-3.9	-19.1	103.8	36.3	-4.1
II(A)1	6.00	2.64	7.00	100.44	2.35	3.15	4.00	-35.7	106.1	-5.5	-19.6	107.7	36.4	-8.3
	3.00	2.45	4.00	84.91	2.44	3.08	2.00	-17.9	98.4	-3.2	-16.6	111.5	35.6	-4.1
II(A)2	5.00	2.48	4.00	<b>99.64</b>	2.32	3.24	4.00	<b>-29.8</b>	<b>99.7</b>	<b>-3.2</b>	<b>-19.5</b>	106.3	37.5	<b>-8.3</b>
	6.00	2.63	6.00	<b>97.61</b>	2.36	3.21	0.00	-35.7	105.4	-4.7	<b>-19.1</b>	108.2	37.1	0.0
II(B)1	6.00	2.64	5.00	97.58	2.31	3.13	2.00	-35.7	106.2	-3.9	-19.1	105.9	36.2	-4.1
	6.00	2.65	5.00	97.24	2.28	3.15	2.00	-35.7	106.4	-3.9	-19.0	104.5	36.3	-4.1
II(B)2	6.00	2.63	6.00	99.47	2.28	3.16	2.00	-35.7	105.6	-4.7	-19.5	104.3	36.5	-4.1
	3.00	2.45	7.00	85.63	2.35	3.12	2.00	-17.9	98.3	-5.5	-16.7	107.6	36.0	-4.1
II(B)3	6.00	2.64	5.00	<b>98.09</b>	2.28	3.13	2.00	-35.7	106.2	-3.9	<b>-19.2</b>	104.2	36.1	-4.1
	3.00	2.45	7.00	<b>85.29</b>	2.35	3.16	2.00	-17.9	98.3	-5.5	<b>-16.7</b>	107.4	36.6	-4.1
II(D)1	6.00	2.64	5.00	98.49	2.30	3.12	2.00	-35.7	105.9	-3.9	-19.3	105.1	36.1	-4.1
	6.00	2.67	5.00	96.04	2.29	3.10	2.00	-35.7	107.2	-3.9	-18.8	104.8	35.8	-4.1
II(D)2	6.00	2.63	7.00	<b>99.44</b>	2.33	3.17	2.00	-35.7	105.7	-5.5	<b>-19.5</b>	106.5	36.7	-4.1
	4.00	2.75	6.00	90.87	2.30	3.20	3.00	-23.8	110.5	-4.7	-17.8	105.3	37.0	-6.2
II(F)5	3.00	2.45	7.00	<b>85.74</b>	2.34	3.12	2.00	-17.9	98.3	-5.5	<b>-16.8</b>	107.3	36.0	-4.1
	6.00	2.65	5.00	<b>97.65</b>	2.26	3.14	2.00	-35.7	106.5	-3.9	<b>-19.1</b>	103.4	36.3	-4.1
III(A)1	6.00	2.64	5.00	97.68	2.30	3.15	2.00	-35.7	106.1	-3.9	-19.1	105.5	36.4	-4.1
	6.00	2.64	5.00	97.68	2.30	3.15	2.00	-35.7	106.1	-3.9	-19.1	105.5	36.4	-4.1
III(A)2	6.00	2.61	7.00	<b>100.89</b>	2.31	3.12	2.00	-35.7	104.8	-5.5	<b>-19.7</b>	105.7	36.0	-4.1
	3.00	2.49	6.00	84.31	2.39	3.14	2.00	-17.9	99.9	-4.7	<b>-16.5</b>	109.5	36.3	-4.1
III(E)1	6.0	2.67	5.00	<b>96.58</b>	2.27	3.14	2.00	-35.7	107.0	-3.9	<b>-18.9</b>	103.9	36.3	-4.1
	6.00	2.66	5.00	<b>97.11</b>	2.28	3.15	2.00	-35.7	106.8	-3.9	<b>-19.0</b>	104.6	36.3	-4.1
III(E)2	6.00	2.67	5.00	95.95	2.26	3.17	2.00	-35.7	107.4	-3.9	-18.8	103.6	36.6	-4.1
	3.00	2.46	7.00	84.90	2.34	3.15	2.00	-17.9	98.8	-5.5	-16.6	107.4	36.4	-4.1
III(F)1	6.00	2.67	5.00	96.79	2.30	3.10	2.00	-35.7	107.0	-3.9	-18.9	105.1	35.9	-4.1
	6.00	2.67	5.00	96.69	2.30	3.10	2.00	-35.7	107.0	-3.9	-18.9	105.1	35.8	-4.1
III(F)3	6.00	2.67	5.00	96.36	2.28	3.11	2.00	-35.7	107.2	-3.9	-18.8	104.5	36.0	-4.1
	3.00	2.45	6.00	85.47	2.32	3.13	2.00	-17.9	98.5	-4.7	-16.7	106.4	36.2	-4.1

Table S5 The geometric descriptors and their contribution to the  $^{23}\text{Na}$  NMR  $\sigma$  parameters for MD NMR calculation in CHA(17). The cases discussed in the text are in bold.

CHA(17)	Geometrical descriptors							Contribution to the $^{23}\text{Na}$ NMR $\sigma$ (ppm)						
	CN <sub>Na-O</sub>	d <sub>Na-O</sub> (Å)	CN <sub>Na-Si</sub>	$\alpha_{O-Na-O}$ (°)	d <sub>Na-O</sub> <sup>min</sup> (Å)	d <sub>Na-Si</sub> <sup>min</sup> (Å)	CN <sub>Na-O(Al)</sub>	CN <sub>Na-O</sub>	d <sub>Na-O</sub> (Å)	CN <sub>Na-Si</sub>	$\alpha_{O-Na-O}$ (°)	d <sub>Na-O</sub> <sup>min</sup> (Å)	d <sub>Na-Si</sub> <sup>min</sup> (Å)	CN <sub>Na-O(Al)</sub>
I(A)1	5.95	2.65	6.32	100.60	2.23	3.11	4.00	-35.4	106.2	-5.0	-19.7	102.3	36.0	-8.2
	3.63	2.61	5.81	91.27	2.29	3.10	2.00	-21.6	104.6	-4.6	-17.9	104.7	35.8	-4.1
I(A)3	5.79	2.66	4.89	97.83	2.24	3.14	4.00	-34.5	106.6	-3.9	-19.1	102.4	36.3	-8.3
	5.95	2.67	6.24	95.75	2.31	3.15	0.00	-35.4	107.1	-4.9	-18.7	105.5	36.4	0.0
I(C)1	<b>5.89</b>	<b>2.67</b>	<b>5.66</b>	<b>96.58</b>	<b>2.23</b>	<b>3.15</b>	<b>2.00</b>	<b>-35.1</b>	<b>107.3</b>	<b>-4.5</b>	<b>-18.9</b>	<b>102.2</b>	<b>36.4</b>	<b>-4.1</b>
	5.01	2.67	5.60	94.02	2.26	3.14	2.03	-29.8	107.2	-4.4	-18.4	103.6	36.3	-4.2
I(C)3	5.80	2.67	5.49	95.69	2.25	3.07	2.00	-34.5	107.3	-4.3	-18.7	102.9	35.5	-4.1
	5.75	2.67	5.58	95.94	2.23	3.16	2.02	-34.2	107.2	-4.4	-18.8	102.3	36.5	-4.
I(E)1	5.98	2.66	6.38	97.91	2.26	3.11	2.00	-35.6	107.0	-5.0	-19.2	103.3	36.0	-4.1
	3.51	2.53	4.43	91.84	2.29	2.99	3.46	-20.9	101.5	-3.5	-18.0	105.0	34.5	-7.1
I(E)3	5.99	2.67	6.15	97.66	2.24	3.11	2.00	-35.7	107.0	-4.9	-19.1	102.4	36.0	-4.1
	5.87	2.67	5.76	96.77	2.25	3.11	2.00	-35.0	107.0	-4.5	-18.9	103.1	36.0	-4.1
I(E)4	5.94	2.67	5.85	97.12	2.23	3.13	2.00	-35.4	107.3	-4.6	-19.0	102.3	36.2	-4.1
	3.45	2.57	6.63	89.23	2.28	3.14	2.00	-20.5	103.3	-5.2	-17.5	104.2	36.3	-4.1
I(F)1	<b>5.96</b>	<b>2.65</b>	<b>6.20</b>	<b>97.65</b>	<b>2.25</b>	<b>3.14</b>	<b>2.00</b>	<b>-35.5</b>	<b>106.5</b>	<b>-4.9</b>	<b>-19.1</b>	<b>102.8</b>	<b>36.2</b>	<b>-4.1</b>
	5.91	2.65	6.05	97.03	2.24	3.06	2.00	-35.2	106.2	-4.8	-19.0	102.5	35.3	-4.1
I(F)2	5.95	2.65	6.54	97.97	2.27	3.12	1.99	-35.4	106.3	-5.2	-19.2	103.9	36.1	-4.1
	3.46	2.55	4.49	89.92	2.31	2.99	3.28	-20.6	102.2	-3.5	-17.6	105.7	34.6	-6.8
I(G)1	5.91	2.67	5.81	96.08	2.21	3.12	2.00	-35.2	107.0	-4.6	-18.8	101.3	36.0	-4.1
	5.90	2.66	5.90	96.55	2.21	3.12	2.00	-35.1	106.7	-4.7	-18.9	101.3	36.0	-4.1
II(A)1	5.90	2.64	6.08	100.60	2.28	3.14	4.00	-35.1	105.9	-4.8	-19.7	104.5	36.2	-8.3
	3.69	2.63	4.67	92.35	2.34	3.06	2.20	-21.9	105.6	-3.7	-18.1	107.1	35.3	-4.6
II(A)2	<b>5.59</b>	<b>2.60</b>	<b>4.87</b>	<b>98.59</b>	<b>2.28</b>	<b>3.16</b>	<b>4.00</b>	<b>-33.3</b>	<b>104.4</b>	<b>-3.8</b>	<b>-19.3</b>	<b>104.6</b>	<b>36.5</b>	<b>-8.3</b>
	5.98	2.66	6.30	96.27	2.31	3.15	0.00	-35.6	106.7	-5.0	-18.8	105.6	36.4	0.0
II(B)1	5.91	2.66	5.64	97.20	2.26	3.12	2.00	-35.2	106.7	-4.5	-19.0	103.5	36.1	-4.1
	5.96	2.68	5.59	96.19	2.27	3.15	2.00	-35.5	107.6	-4.4	-18.8	103.7	36.4	-4.1
II(B)2	6.00	2.64	6.75	99.61	2.26	3.13	2.02	-35.7	106.1	-5.3	-19.5	103.3	36.2	-4.2
	3.36	2.57	6.37	88.89	2.29	3.12	1.99	-20.0	103.0	-5.0	-17.4	104.8	36.0	-4.1
II(B)3	<b>5.98</b>	<b>2.65</b>	<b>6.27</b>	<b>98.21</b>	<b>2.25</b>	<b>3.11</b>	<b>2.00</b>	<b>-35.6</b>	<b>106.6</b>	<b>-4.9</b>	<b>-19.2</b>	<b>103.1</b>	<b>36.0</b>	<b>-4.1</b>
	4.08	2.62	6.07	90.19	2.29	3.19	2.07	-24.3	105.1	-4.8	-17.6	105.0	36.8	-4.3
II(D)1	5.95	2.66	6.19	98.04	2.25	3.10	2.00	-35.4	106.6	-4.9	-19.2	103.0	35.9	-4.1
	5.85	2.66	6.02	97.12	2.24	3.10	2.00	-34.8	106.8	-4.7	-19.0	102.7	35.8	-4.1
II(D)2	<b>6.00</b>	<b>2.66</b>	<b>6.52</b>	<b>98.70</b>	<b>2.27</b>	<b>3.11</b>	<b>2.00</b>	<b>-35.7</b>	<b>106.6</b>	<b>-5.1</b>	<b>-19.3</b>	<b>103.8</b>	<b>36.0</b>	<b>-4.1</b>
	3.94	2.69	4.66	92.26	2.29	3.07	2.73	-23.5	108.1	-3.7	-18.0	104.9	35.5	-5.6
II(F)5	3.79	2.62	6.22	89.16	2.27	3.12	2.15	-22.6	105.1	-4.9	-17.4	103.7	36.1	-4.4
	5.95	2.67	6.03	97.13	2.24	3.13	2.00	-35.4	107.2	-4.8	-19.0	102.6	36.2	-4.1
III(A)1	5.93	2.65	5.80	97.43	2.27	3.13	2.00	-35.3	106.5	-4.6	-19.1	103.8	36.1	-4.1
	5.85	2.64	5.62	97.16	2.28	3.13	2.00	-34.8	106.1	-4.4	-19.0	104.4	36.2	-4.1
III(A)2	<b>5.97</b>	<b>2.64</b>	<b>6.99</b>	<b>100.19</b>	<b>2.27</b>	<b>3.11</b>	<b>2.00</b>	<b>-35.5</b>	<b>105.8</b>	<b>-5.5</b>	<b>-19.6</b>	<b>103.8</b>	<b>35.9</b>	<b>-4.1</b>
	3.48	2.62	5.79	88.86	2.33	3.12	1.93	-20.7	105.1	-4.6	-17.4	106.7	36.0	-4.1
III(E)1	5.95	2.67	5.70	96.73	2.25	3.12	1.99	-35.4	107.2	-4.5	-18.9	102.9	36.1	-4.1
	5.93	2.67	5.77	97.02	2.25	3.13	2.00	-35.3	107.1	-4.5	-19.0	103.1	36.1	-4.1
III(E)2	5.94	2.66	5.84	97.48	2.24	3.10	2.00	-35.4	106.8	-4.6	-19.1	102.7	35.9	-4.1
	3.48	2.59	6.40	90.42	2.29	3.14	1.99	-20.7	104.1	-5.0	-17.7	104.9	36.3	-4.1
III(F)1	5.91	2.66	6.14	97.28	2.25	3.10	2.00	-35.2	106.7	-4.8	-19.0	102.9	35.9	-4.1
	5.93	2.67	5.92	96.96	2.25	3.11	2.00	-35.3	107.0	-4.7	-19.0	102.9	35.9	-4.1
III(F)3	5.96	2.68	5.68	96.79	2.25	3.14	2.00	-35.5	107.5	-4.5	-18.9	103.2	36.3	-4.1
	3.55	2.58	5.94	90.87	2.26	3.10	2.03	-21.2	103.5	-4.7	-17.8	103.6	35.8	-4.2

## 6 $^{23}\text{Na}$ NMR for CHA(35)

Table S6 Static  $^{27}\text{Al}$  and  $^{23}\text{Na}$  NMR parameters of CHA(35). Note the Na positions are shown in the Figure S2.

Na positions	$^{23}\text{Na}$			$^{27}\text{Al}$		
	$\delta_{\text{Na}}$ (ppm)	$C_{Q_{\text{Na}}}$ (MHz)	$\eta_{Q_{\text{Na}}}$	$\delta_{\text{Al}}$ (ppm)	$C_{Q_{\text{Al}}}$ (MHz)	$\eta_{Q_{\text{Al}}}$
SII	-8.5	4.0	0.26	59.6	7.6	0.75
SIII	-21.1	3.5	0.42	61.1	7.0	0.75
SIII'	-21.5	3.4	0.33	62.6	5.9	0.73

## 7 $^{23}\text{Na}$ NMR for CHA(17)

Table S7  $^{23}\text{Na}$  NMR parameters of CHA(17).

Structure	Static						MD					
	$\delta_{\text{Na}1}$ (ppm)	$C_{Q_{\text{Na}1}}$ (MHz)	$\eta_{Q_{\text{Na}1}}$	$\delta_{\text{Na}2}$ (ppm)	$C_{Q_{\text{Na}2}}$ (MHz)	$\eta_{Q_{\text{Na}2}}$	$\delta_{\text{isoNa}1}$ (ppm)	$C_{Q_{\text{Na}1}}$ (MHz)	$\eta_{Q_{\text{Na}1}}$	$\delta_{\text{Na}2}$ (ppm)	$C_{Q_{\text{Na}2}}$ (MHz)	$\eta_{Q_{\text{Na}2}}$
I(A)1	-4.1	4.5	0.49	-21.4	3.5	0.61	-1.7	3.8	0.76	-19.7	-3.2	0.93
I(A)2	-2.8	4.8	0.49	-21.8	3.5	0.37						
I(A)3	-3.5	4.3	0.68	-12.6	3.7	0.30	-4.3	-4.6	0.83	-13.9	3.9	0.80
I(B)1	-6.2	4.5	0.26	-23.5	3.3	0.31						
I(B)2	-5.5	4.2	0.51	-12.0	3.6	0.28						
I(B)3	-1.6	4.7	0.37	-22.4	3.3	0.10						
I(C)1	-9.1	4.0	0.60	-6.1	4.1	0.23	-8.9	-4.0	0.89	-12.6	3.6	0.77
I(C)2	-7.2	4.4	0.27	-18.6	3.6	0.75	-7.0	4.9	0.30	-15.0	3.3	0.54
I(C)3	-5.2	4.4	0.26	-20.8	3.5	0.31	-7.3	4.6	0.84	-10.0	2.9	0.37
I(D)1	-7.6	3.9	0.33	-7.5	4.0	0.37						
I(D)2	-6.7	4.2	0.32	-21.1	3.5	0.41						
I(D)3	-6.4	4.3	0.31	-19.2	3.6	0.58						
I(D)4	-8.5	4.4	0.35	-19.4	3.6	0.55						
I(D)5	-7.2	4.2	0.35	-20.9	3.4	0.31						
I(E)1	-9.8	3.9	0.40	-16.1	-3.8	0.98	-8.3	4.7	0.16	-15.1	3.8	0.79
I(E)2	-6.3	4.3	0.25	-17.7	4.1	0.33						
I(E)3	-8.4	3.9	0.37	-7.9	3.8	0.30	-7.0	3.6	0.75	-7.7	-5.5	0.66
I(E)4	-8.0	4.0	0.47	-20.4	3.7	0.11	-8.2	3.8	0.36	-19.3	4.0	0.77
I(E)5	-8.9	3.8	0.39	-22.4	3.5	0.28						
I(E)6	-23.5	3.4	0.38	-22.5	3.5	0.32						
I(F)1	-7.6	3.7	0.31	-5.9	3.9	0.25	-6.8	3.1	0.71	-4.4	4.4	0.49
I(F)2	-9.6	4.1	0.27	-17.3	-3.9	0.81	-8.6	-4.9	0.88	-17.9	-4.2	0.97
I(F)3	-4.6	4.4	0.32	-19.6	3.4	0.61						
I(G)1	-8.6	3.9	0.61	-8.5	3.9	0.60	-6.7	2.4	0.97	-6.8	-5.9	0.77
I(G)2	-19.7	3.7	0.32	-19.8	3.7	0.31						
I(G)3	-19.0	3.7	0.47	-19.0	3.7	0.48	-17.9	3.6	0.71	-17.9	3.9	0.12
I(G)4	-8.7	3.7	0.47	-20.2	3.6	0.40						
I(G)5	-18.4	3.8	0.39	-19.0	3.8	0.34						
I(H)1	-10.0	4.0	0.55	-16.6	3.8	0.84						
I(H)2	-24.7	3.3	0.36	-15.8	3.7	0.92						

Continued on next page

Continued on next page

II(J)6	-19.2	3.6	0.60	-19.3	3.6	0.70							
II(J)7	-20.9	3.6	0.21	-20.1	3.4	0.62							
II(J)8	-21.6	3.4	0.34	-19.1	3.6	0.41							
II(K)1	-9.0	3.4	0.59	-8.4	4.1	0.25							
II(K)2	-7.1	3.8	0.54	-22.4	3.6	0.38							
II(K)3	-7.2	3.8	0.54	-22.5	3.6	0.38							
II(K)4	-9.5	3.4	0.68	-20.6	3.5	0.44							
II(K)5	-9.9	3.4	0.70	-20.8	3.5	0.44							
II(L)1	-9.3	3.9	0.64	-8.5	4.2	0.56							
III(A)1	-8.6	4.2	0.31	-8.6	4.2	0.31	-7.8	4.9	0.28	-8.5	2.5	0.56	
III(A)2	-7.6	4.3	0.24	-25.5	3.2	0.18	-6.5	-4.3	0.97	-23.5	2.3	0.61	
III(B)1	-9.1	3.6	0.53	-8.1	4.0	0.29							
III(B)2	-9.8	3.7	0.61	-22.2	3.4	0.27							
III(C)1	-9.3	3.4	0.59	-10.2	4.0	0.35							
III(C)2	-9.6	3.5	0.60	-20.0	3.6	0.49							
III(C)3	-9.2	4.0	0.28	-20.9	3.5	0.50							
III(C)4	-20.8	3.6	0.32	-21.2	3.4	0.52							
III(C)5	-7.6	3.9	0.49	-18.7	3.8	0.61							
III(D)1	-10.2	3.9	0.37	-9.0	3.4	0.58							
III(D)2	-9.0	4.0	0.50	-20.9	3.6	0.33							
III(D)3	-9.3	4.0	0.28	-21.0	3.5	0.50							
III(D)4	-20.8	3.6	0.32	-21.1	3.4	0.52							
III(D)5	-21.3	3.5	0.43	-21.4	3.5	0.35							
III(D)6	-21.7	3.4	0.35	-21.3	3.5	0.38							
III(E)1	-9.6	3.6	0.72	-9.5	4.0	0.32	-8.5	-4.3	0.93	-7.1	4.2	0.60	
III(E)2	-9.7	3.5	0.83	-22.0	3.5	0.32	-6.6	4.2	0.34	-20.8	3.3	0.65	
III(E)3	-21.7	3.4	0.44	-22.5	3.4	0.29							
III(F)1	-9.7	3.7	0.45	-9.5	3.7	0.43	-7.7	4.4	0.55	-7.7	-4.3	0.86	
III(F)2	-7.3	4.0	0.49	-22.2	3.5	0.42							
III(F)3	-9.4	3.7	0.54	-20.8	3.6	0.45	-8.9	4.8	0.21	-18.0	3.9	0.07	
III(F)4	-22.8	3.4	0.34	-22.9	3.4	0.32							
III(G)1	-9.7	3.6	0.68	-10.4	3.8	0.79							
III(G)2	-10.7	3.7	0.89	-22.0	3.5	0.32							
III(G)3	-10.1	3.5	0.68	-20.7	3.6	0.41							
III(G)4	-21.9	3.5	0.34	-21.4	3.5	0.45							
III(G)5	-20.7	3.4	0.47	-22.4	3.5	0.36							
III(G)6	-8.2	4.2	0.78	-19.4	3.7	0.52							
III(G)7	-20.4	3.6	0.47	-21.0	3.5	0.50							
III(H)1	-9.6	3.7	0.35	-9.8	3.7	0.35							
III(H)2	-10.2	3.7	0.79	-21.8	3.4	0.28							
IV(A)1	-9.7	3.7	0.47	-8.6	3.8	0.26	-7.4	4.6	0.93	-7.4	3.9	0.13	
IV(A)2	-8.9	3.7	0.35	-20.2	3.6	0.43							
IV(A)3	-9.9	3.5	0.67	-20.1	3.6	0.48							
IV(A)4	-21.2	3.4	0.53	-21.2	3.5	0.40							
IV(A)5	-5.3	4.2	0.17	-18.9	3.7	0.60							
IV(A)6	-21.4	3.5	0.40	-21.0	3.5	0.45							
IV(B)1	-9.6	3.6	0.68	-10.6	3.6	0.81							
IV(B)2	-10.1	3.5	0.85	-22.0	3.5	0.31							
IV(B)3	-10.4	3.5	0.90	-21.8	3.5	0.30							

Continued on next page

IV(B)4	-21.7	3.5	0.21	-21.9	3.5	0.22
IV(B)5	-20.1	3.5	0.47	-22.0	3.5	0.32

---

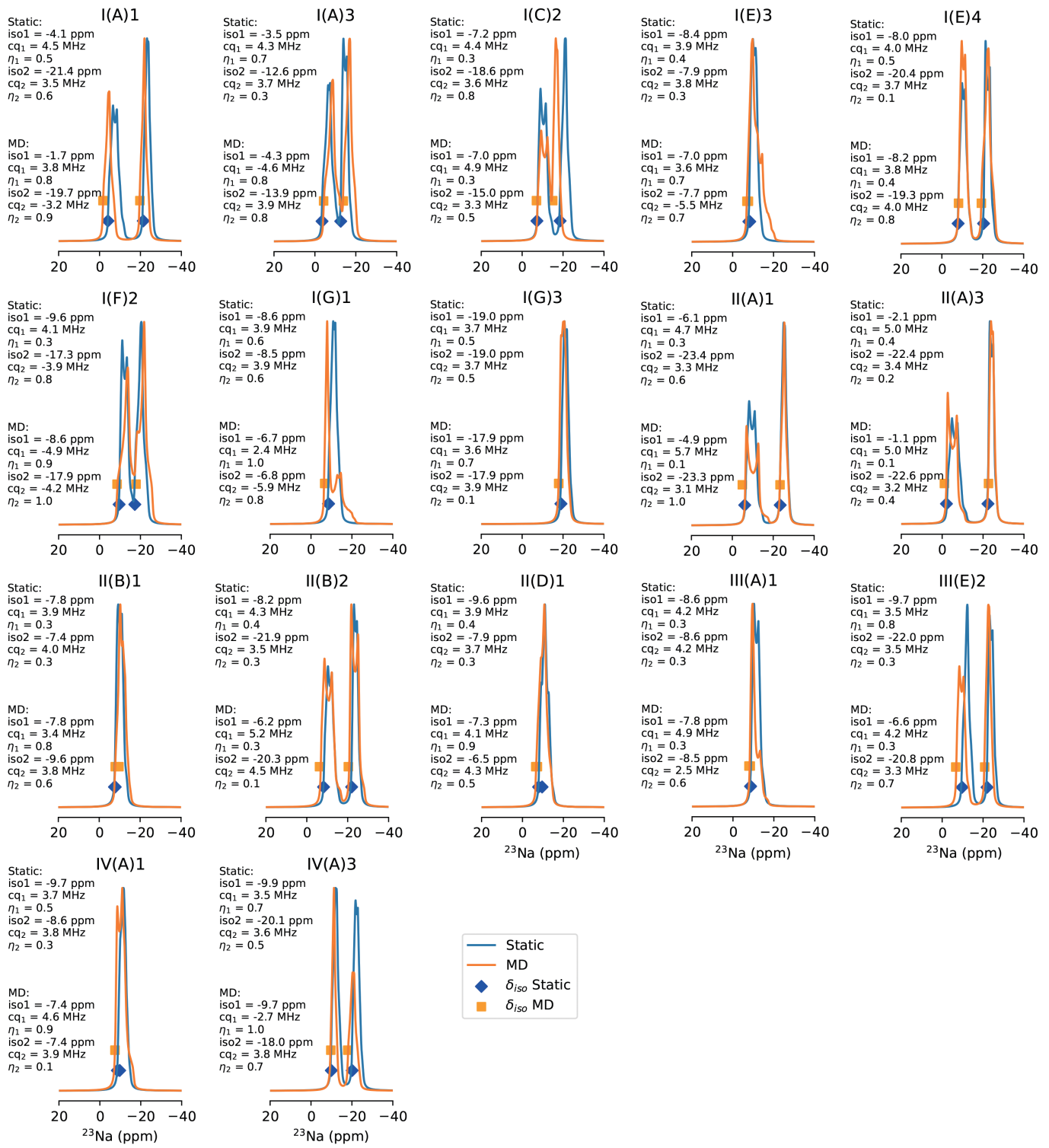


Fig. S8 Simulated <sup>23</sup>Na NMR spectra of static and time-averaged CHA17 models with distinct Na/Al configurations, which combined with those presented in Figure 4 in the main text, make up the full set of calculated CHA(17) spectra.

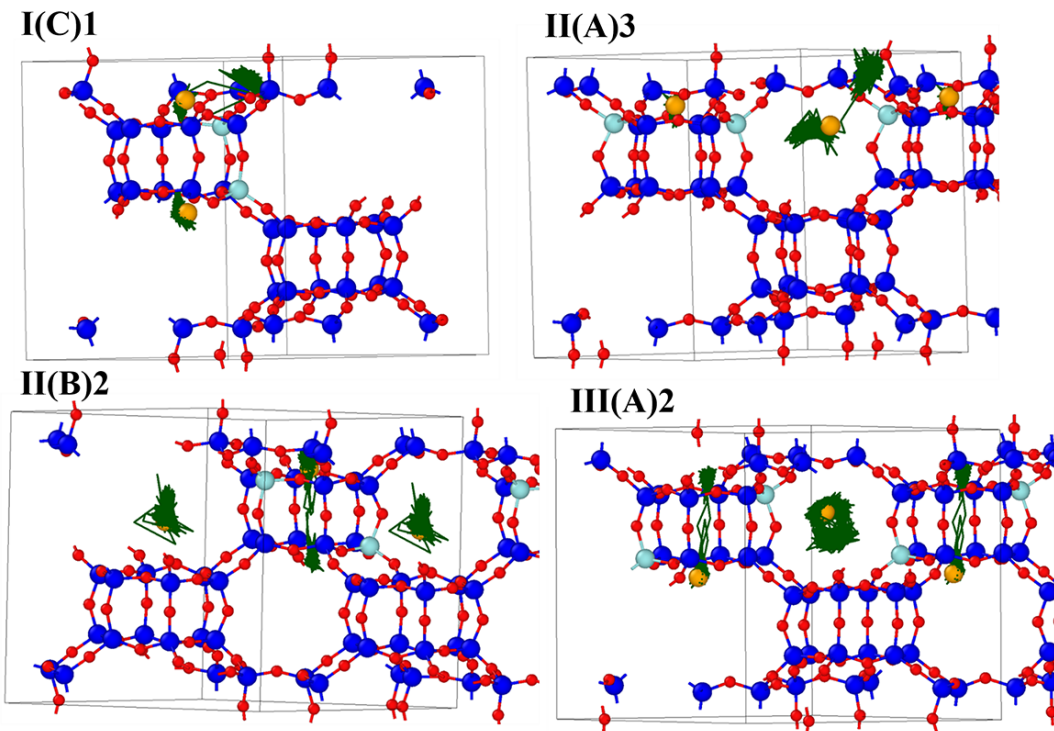


Fig. S9 The trajectories of the motion of Na of CHA(17) in I(C), II(A), II(B), and III(A) cases, in which the  $\text{Na}^+$  migrated to different sites. Note: the trajectory lines are in green.

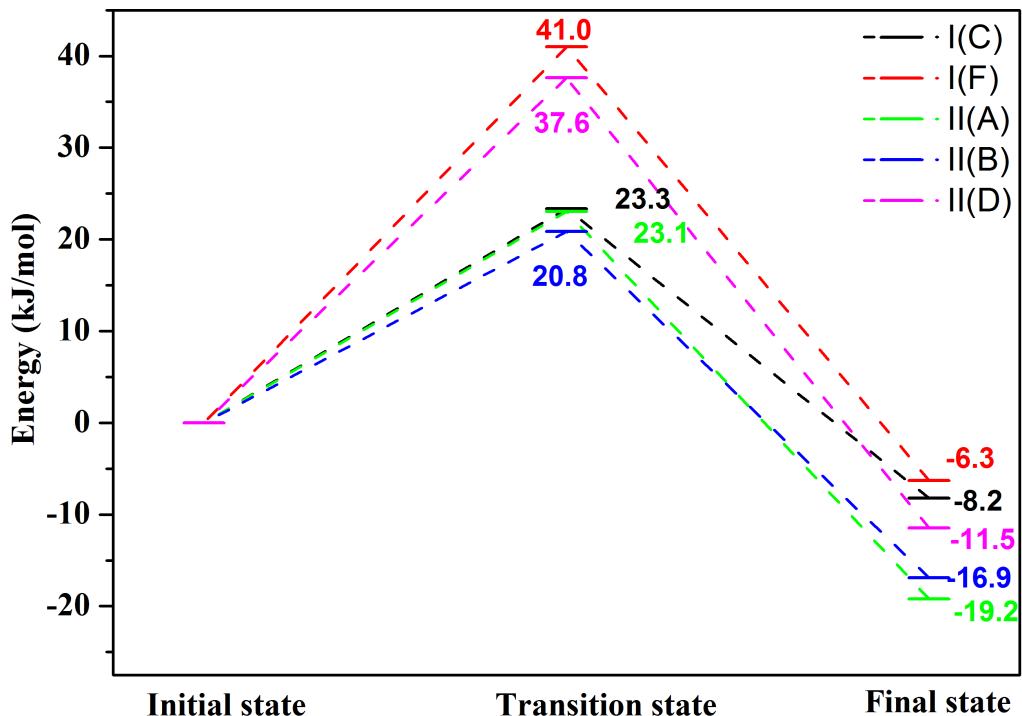


Fig. S10 The energy barrier of two stated in I(C), I(F), II(A), II(B) and II(D) cases with NNP NEB( nudged elastic band) method. The initial states are the higher energy cases with one 6-ring  $\text{Na}^+$  and one 8-ring(I(C)3, I(F)2, II(A)3, II(B)3 and II(D)2), and the final states are the corresponding minimal state with two 6-ring  $\text{Na}^+$ .

## 8 $^{27}\text{Al}$ NMR chemical shifts for CHA(17)

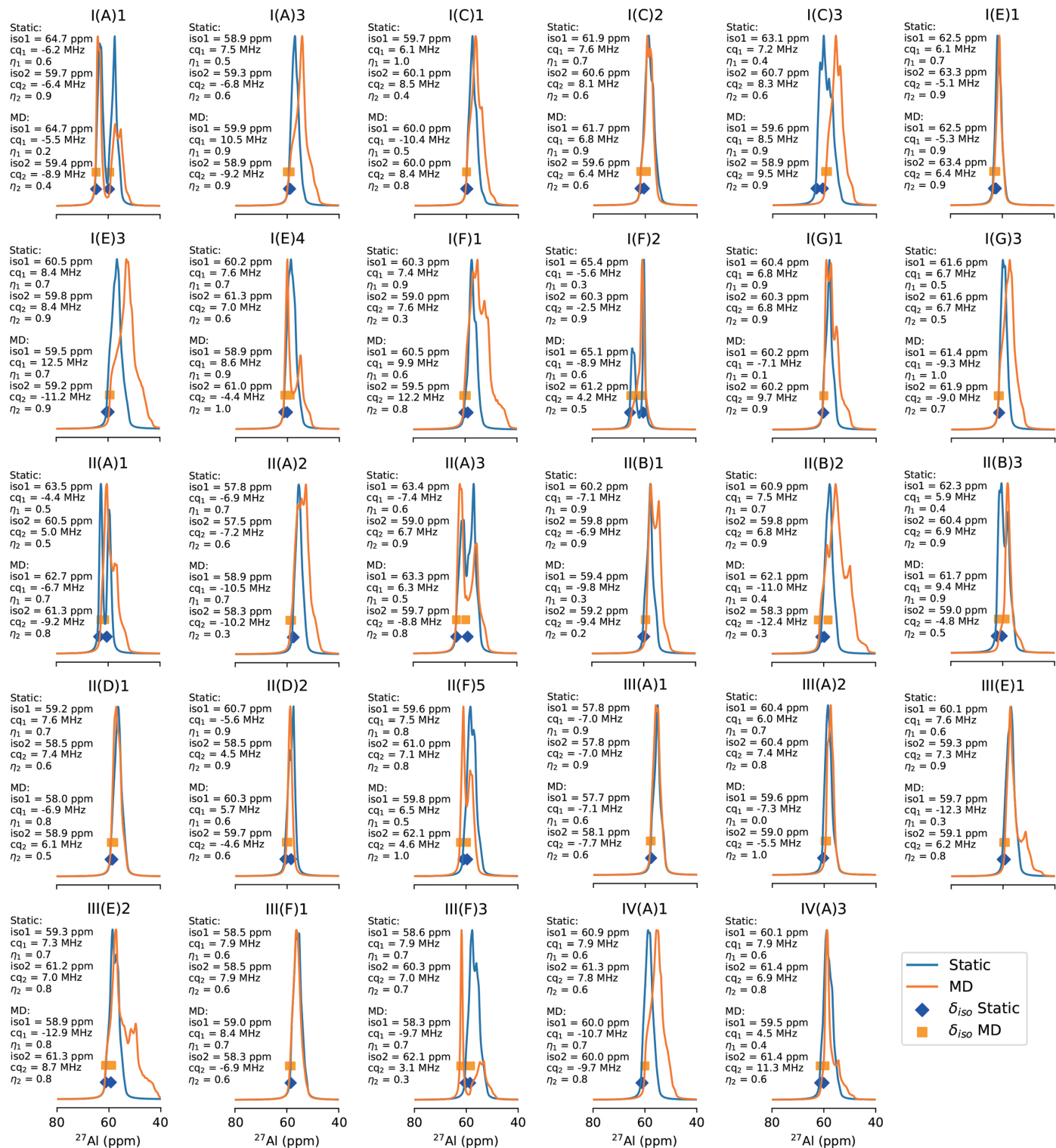


Fig. S11 Simulated  $^{27}\text{Al}$  NMR spectra of static and time-averaged CHA17 models with distinct Na/Al configurations considered in Figure 4 and S8.

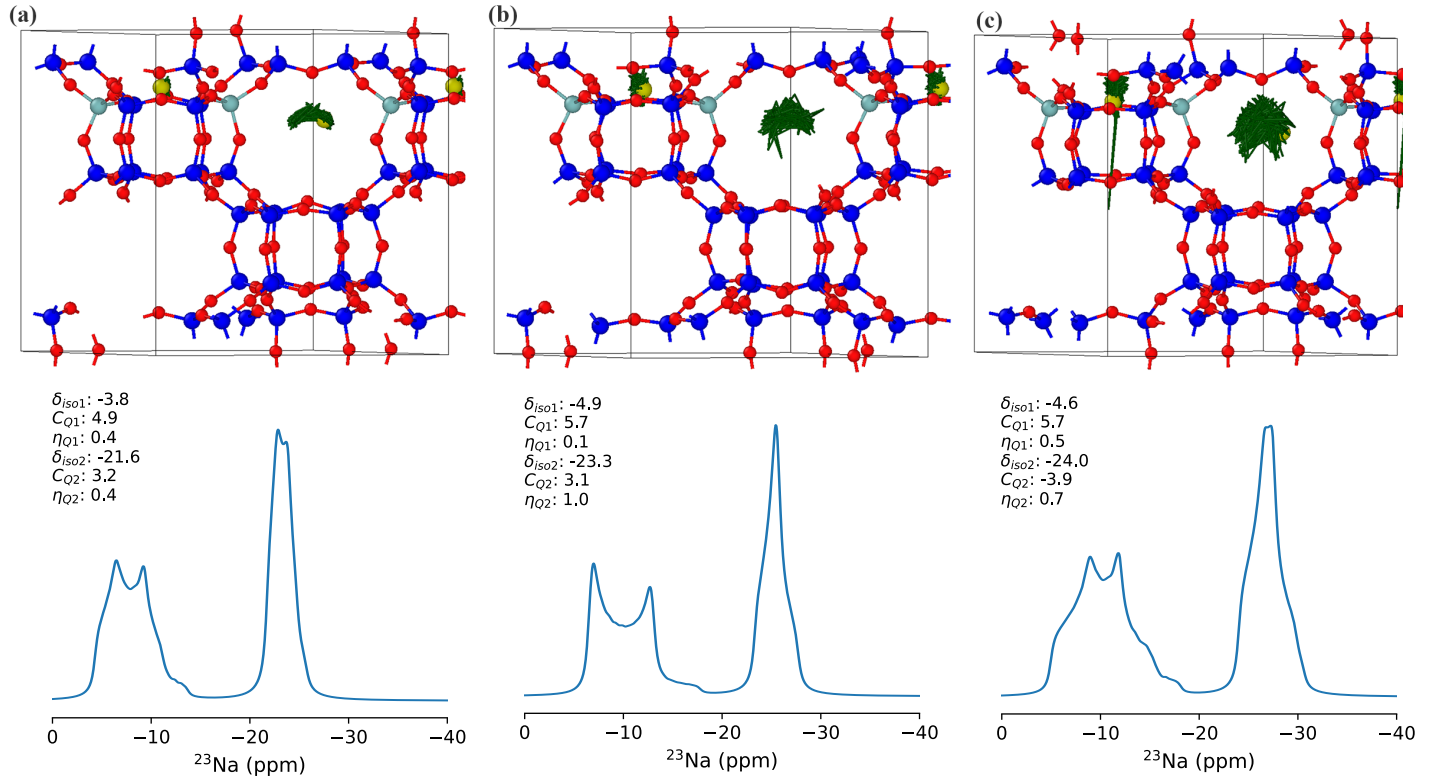


Fig. S12 Trajectories of  $\text{Na}^+$  at different temperatures of CHA(17) with Al-Si<sub>2</sub>-Al sequence in 6MR and respective simulated  $^{23}\text{Na}$  spectra. (a), (b), and (c) show the trajectories at 150, 350, and 550 K, respectively. The path indicates the  $\text{Na}$  atom traces, only the initial position of the rest of the atoms is shown.

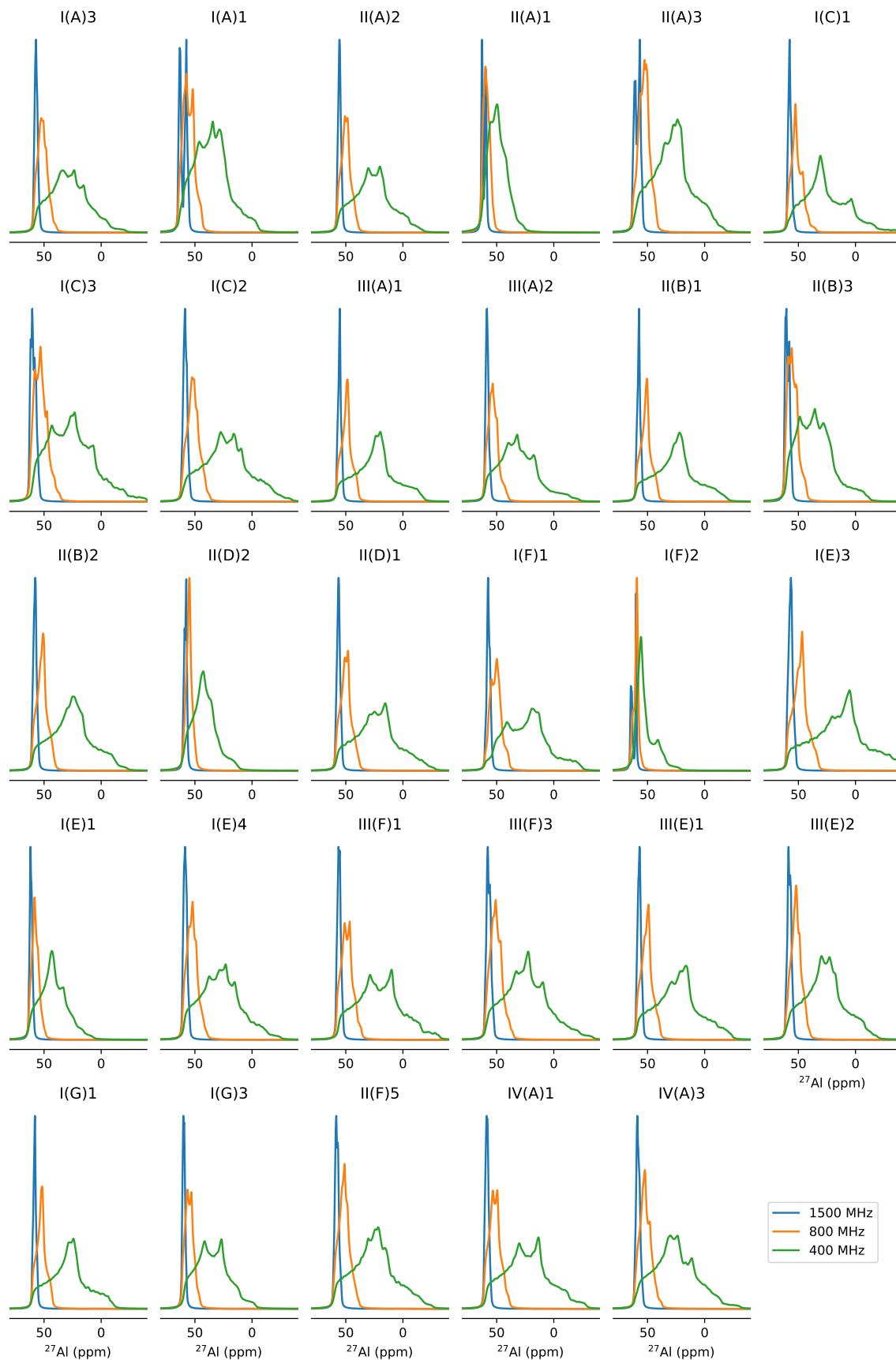


Fig. S13  $^{27}\text{Al}$  NMR spectra of static CHA17 models at different magnetic fields, ranging from 400 to 1500 MHz.

Table S8  $^{27}\text{Al}$  NMR parameters of CHA(17).

Structure	Static						MD					
	$\delta_{\text{Al}1}$ (ppm)	$C_{Q_{\text{Al}1}}$ (MHz)	$\eta_{Q_{\text{Al}1}}$	$\delta_{\text{Al}2}$ (ppm)	$C_{Q_{\text{Al}2}}$ (MHz)	$\eta_{Q_{\text{Al}2}}$	$\delta_{\text{Al}1}$ (ppm)	$C_{Q_{\text{Al}1}}$ (MHz)	$\eta_{Q_{\text{Al}1}}$	$\delta_{\text{Al}2}$ (ppm)	$C_{Q_{\text{Al}2}}$ (MHz)	$\eta_{Q_{\text{Al}2}}$
I(A)1	64.7	-6.2	0.55	59.7	-6.4	0.95	64.7	-5.5	0.15	59.4	-8.9	0.37
I(A)2	65.7	-7.3	0.38	59.4	7.2	0.87						
I(A)3	58.9	7.5	0.55	59.3	-6.8	0.62	59.9	10.5	0.92	58.8	-9.2	0.89
I(B)1	64.0	-4.5	0.58	59.7	7.8	0.43						
I(B)2	59.1	-6.9	0.69	58.8	6.9	0.85						
I(B)3	64.2	-7.6	0.86	60.3	7.7	0.50						
I(C)1	59.7	6.1	0.99	60.1	8.5	0.42	60.0	-10.4	0.49	60.0	8.4	0.84
I(C)2	61.8	7.6	0.73	60.5	8.1	0.60	61.7	6.8	0.92	59.6	6.4	0.63
I(C)3	63.1	7.2	0.41	60.7	8.3	0.59	59.6	8.5	0.92	58.9	9.5	0.94
I(D)1	59.9	9.0	0.31	59.8	-6.5	0.97						
I(D)2	62.9	5.3	0.98	59.7	6.0	0.99						
I(D)3	60.6	7.4	0.96	60.3	7.8	0.97						
I(D)4	60.6	8.5	0.41	60.8	7.8	0.75						
I(D)5	60.7	8.7	0.45	62.9	7.0	0.71						
I(E)1	62.5	6.1	0.66	63.3	-5.1	0.93	62.5	-5.3	0.92	63.4	6.4	0.94
I(E)2	62.8	6.7	0.92	62.0	-7.5	0.76						
I(E)3	60.5	8.4	0.69	59.7	8.4	0.94	59.5	12.5	0.74	59.2	-11.2	0.86
I(E)4	60.1	7.6	0.68	61.2	7.0	0.57	58.9	8.6	0.91	61.0	-4.4	0.98
I(E)5	63.3	-6.6	0.87	60.6	-8.5	0.85						
I(E)6	61.5	6.9	0.72	65.1	5.8	0.36						
I(F)1	60.3	7.4	0.95	59.0	7.6	0.25	60.5	9.9	0.61	59.5	12.2	0.84
I(F)2	65.4	-5.6	0.31	60.3	-2.5	0.91	65.1	-8.9	0.62	61.2	4.2	0.49
I(F)3	62.3	6.0	0.93	62.8	-7.5	0.84						
I(G)1	60.4	6.8	0.87	60.3	6.8	0.87	60.2	-7.1	0.15	60.2	9.7	0.92
I(G)2	61.9	5.3	0.82	61.8	5.3	0.84						
I(G)3	61.6	6.7	0.50	61.6	6.7	0.50	61.4	-9.3	0.96	61.9	-9.0	0.71
I(G)4	58.9	8.7	0.95	62.7	7.0	0.24						
I(G)5	62.3	5.4	0.86	60.9	7.1	0.45						
I(H)1	62.4	5.6	0.63	63.4	4.9	1.00						
I(H)2	65.8	5.5	0.05	63.3	4.5	0.67						
I(H)3	59.8	7.4	0.65	61.6	7.0	0.47						
I(H)4	62.5	6.6	0.99	61.6	-7.1	0.90						
I(H)5	59.7	7.9	0.74	59.5	8.7	0.86						
I(H)6	62.4	7.2	0.78	64.9	5.9	0.20						
I(H)7	63.5	6.6	0.88	60.1	8.3	1.00						
I(I)1	58.3	7.8	0.18	59.9	6.9	0.96						
I(I)2	62.3	-7.3	0.94	62.8	-6.4	0.98						
II(A)1	63.5	-4.4	0.45	60.5	5.0	0.46	62.7	-6.7	0.73	61.3	-9.2	0.80
II(A)2	57.8	-6.9	0.73	57.5	-7.2	0.62	58.9	-10.5	0.70	58.2	-10.2	0.27
II(A)3	63.4	-7.4	0.62	59.0	6.7	0.88	63.3	6.3	0.48	59.7	-8.8	0.82
II(B)1	60.2	-7.1	0.95	59.8	-6.9	0.86	59.4	-9.8	0.29	59.2	-9.4	0.22
II(B)2	60.9	7.5	0.66	59.8	6.8	0.94	62.1	-11.0	0.42	58.3	-12.4	0.31

Continued on next page

II(B)3	62.3	5.9	0.42	60.3	6.9	0.87	61.7	9.4	0.86	59.0	-4.8	0.49
II(C)1	59.7	7.7	0.56	59.5	7.3	0.68						
II(C)2	61.0	8.1	0.53	59.8	8.0	0.56						
II(C)3	63.9	5.2	0.19	59.2	7.1	0.67						
II(C)4	60.0	8.3	0.40	60.0	8.0	0.68						
II(D)1	59.2	7.6	0.74	58.5	7.4	0.64	58.0	-6.9	0.77	58.9	6.1	0.49
II(D)2	60.7	-5.6	0.86	58.5	4.5	0.86	60.3	5.7	0.62	59.7	-4.6	0.65
II(D)3	61.0	6.9	0.74	60.0	-7.1	0.90						
II(E)1	59.8	7.4	0.55	59.8	7.3	0.57						
II(F)1	59.5	7.7	0.61	59.5	7.2	0.91						
II(F)2	62.7	5.9	0.83	59.1	-7.4	0.87						
II(F)3	58.6	7.6	0.80	62.5	6.0	0.72						
II(F)4	61.0	6.5	0.63	62.1	5.4	0.95						
II(F)5	59.6	7.5	0.78	61.0	7.1	0.76	59.8	6.5	0.52	62.1	4.6	0.98
II(F)6	62.7	5.9	0.83	59.1	-7.4	0.87						
II(F)7	62.5	6.3	0.82	62.0	5.6	0.50						
II(G)1	60.9	7.4	0.72	59.4	7.4	0.73						
II(G)2	60.2	7.3	0.67	63.3	7.1	0.7						
II(G)3	60.1	8.6	0.55	63.3	5.7	0.72						
II(G)4	63.0	-5.6	0.91	63.4	5.4	0.68						
II(H)1	59.4	8.0	0.8	59.0	7.4	0.89						
II(H)2	59.4	7.6	0.74	61.3	7.0	0.84						
II(H)3	65.3	5.9	0.63	62.0	5.4	0.43						
II(H)4	61.8	-6.7	0.93	62.8	5.4	0.9						
II(H)5	60.9	7.3	0.7	61.6	7.6	0.84						
II(I)1	59.1	7.5	0.81	59.7	8.2	0.56						
II(I)2	58.8	7.2	0.98	62.4	5.7	0.89						
II(I)3	63.0	5.9	0.73	58.8	7.9	0.71						
II(I)4	62.4	-5.2	0.97	60.9	6.4	0.44						
II(I)5	61.3	7.1	0.58	59.6	8.0	0.70						
II(I)6	61.0	6.7	0.67	61.5	6.6	0.59						
II(I)7	62.3	5.4	0.55	62.3	6.2	0.86						
II(J)1	59.2	7.7	0.73	60.5	6.9	0.77						
II(J)2	62.2	6.8	0.60	59.6	6.6	0.76						
II(J)3	62.6	5.5	0.83	59.8	8.1	0.63						
II(J)4	63.1	5.2	0.79	63.3	5.6	0.91						
II(J)5	59.7	7.9	0.84	64.4	6.0	0.71						
II(J)6	62.9	5.3	0.94	61.6	6.7	0.74						
II(J)7	61.3	7.1	0.52	62.4	7.8	0.70						
II(J)8	62.2	7.0	0.58	63.7	5.6	0.45						
II(K)1	58.2	7.5	0.55	59.0	7.5	0.80						
II(K)2	59.4	-6.8	0.94	60.1	6.9	0.82						
II(K)3	59.3	-6.8	0.93	60.0	7.0	0.82						
II(K)4	58.5	7.3	0.81	62.0	5.7	0.81						
II(K)5	58.2	7.3	0.83	61.9	5.7	0.81						
II(L)1	60.2	7.5	0.21	60.5	7.1	0.27						
III(A)1	57.8	-7.0	0.88	57.8	-7.0	0.88	57.7	-7.1	0.58	58.0	-7.7	0.58
III(A)2	60.4	6.0	0.69	60.4	7.4	0.76	59.6	-7.3	0.03	59.0	-5.5	0.95
III(B)1	60.7	7.2	0.96	59.6	7.5	0.60						

Continued on next page

III(B)2	62.6	6.1	0.66	59.4	7.6	0.80								
III(C)1	61.5	7.8	0.55	60.7	7.8	0.49								
III(C)2	63.6	5.6	0.69	59.8	7.7	0.66								
III(C)3	60.8	8.6	0.60	63.4	5.7	0.78								
III(C)4	61.8	6.8	0.51	60.9	6.9	0.73								
III(C)5	61.9	7.3	0.62	58.7	8.5	0.59								
III(D)1	60.7	7.8	0.49	61.6	7.9	0.58								
III(D)2	62.7	7.3	0.65	60.7	7.9	0.71								
III(D)3	63.3	5.7	0.77	60.7	8.6	0.62								
III(D)4	60.8	6.9	0.73	61.8	6.8	0.52								
III(D)5	62.5	-5.1	0.97	61.3	6.5	0.63								
III(D)6	62.9	5.4	0.68	63.0	5.6	0.92								
III(E)1	60.1	7.6	0.62	59.3	7.3	0.88	59.7	-12.3	0.31	59.1	6.2	0.82		
III(E)2	59.2	7.3	0.66	61.2	7.0	0.81	58.9	-12.9	0.79	61.3	8.7	0.85		
III(E)3	61.4	7.0	0.67	62.0	5.9	0.74								
III(F)1	58.5	7.9	0.56	58.5	7.9	0.56	59.0	8.4	0.66	58.3	-6.9	0.64		
III(F)2	59.4	7.4	0.89	61.4	5.8	0.94								
III(F)3	58.5	7.9	0.71	60.3	7.0	0.69	58.3	-9.7	0.66	62.1	3.1	0.33		
III(F)4	61.7	5.5	0.79	62.6	6.0	0.41								
III(G)1	59.2	7.5	0.70	59.3	7.1	0.60								
III(G)2	61.8	6.9	0.66	59.0	7.0	0.58								
III(G)3	59.2	7.7	0.70	62.3	7.3	0.59								
III(G)4	62.4	5.6	0.79	62.1	6.9	0.71								
III(G)5	61.4	6.9	0.65	62.9	5.6	0.53								
III(G)6	63.0	-5.7	0.99	58.2	7.9	0.51								
III(G)7	62.3	5.8	0.97	62.9	5.7	0.94								
III(H)1	59.5	7.0	0.6	60.6	7.5	0.75								
III(H)2	59.4	7.1	0.75	63.1	5.8	0.68								
IV(A)1	60.9	7.9	0.58	61.3	7.8	0.61	60.0	-10.7	0.69	60.0	-9.7	0.8		
IV(A)2	62.0	7.0	0.66	60.2	7.9	0.61								
IV(A)3	60.1	7.9	0.58	61.4	6.9	0.77								
IV(A)4	63.0	5.6	0.87	60.8	6.5	0.87								
IV(A)5	63.8	-5.8	1.00	59.5	8.4	0.64								
IV(A)6	62.6	-5.8	0.91	62.5	-5.8	0.94								
IV(B)1	60.1	7.4	0.65	59.9	7.2	0.71								
IV(B)2	59.5	7.4	0.79	62.2	7.1	0.68								
IV(B)3	61.9	7.1	0.72	59.2	7.2	0.83								
IV(B)4	62.1	7.1	0.64	62.5	7.1	0.62								
IV(B)5	61.6	7.0	0.65	62.7	5.9	0.70								

## 9 Dipolar coupling



Fig. S14  $^{23}\text{Na}$ - $^{23}\text{Na}$  dipolar couplings calculated from static (blue) and MD trajectory (orange).

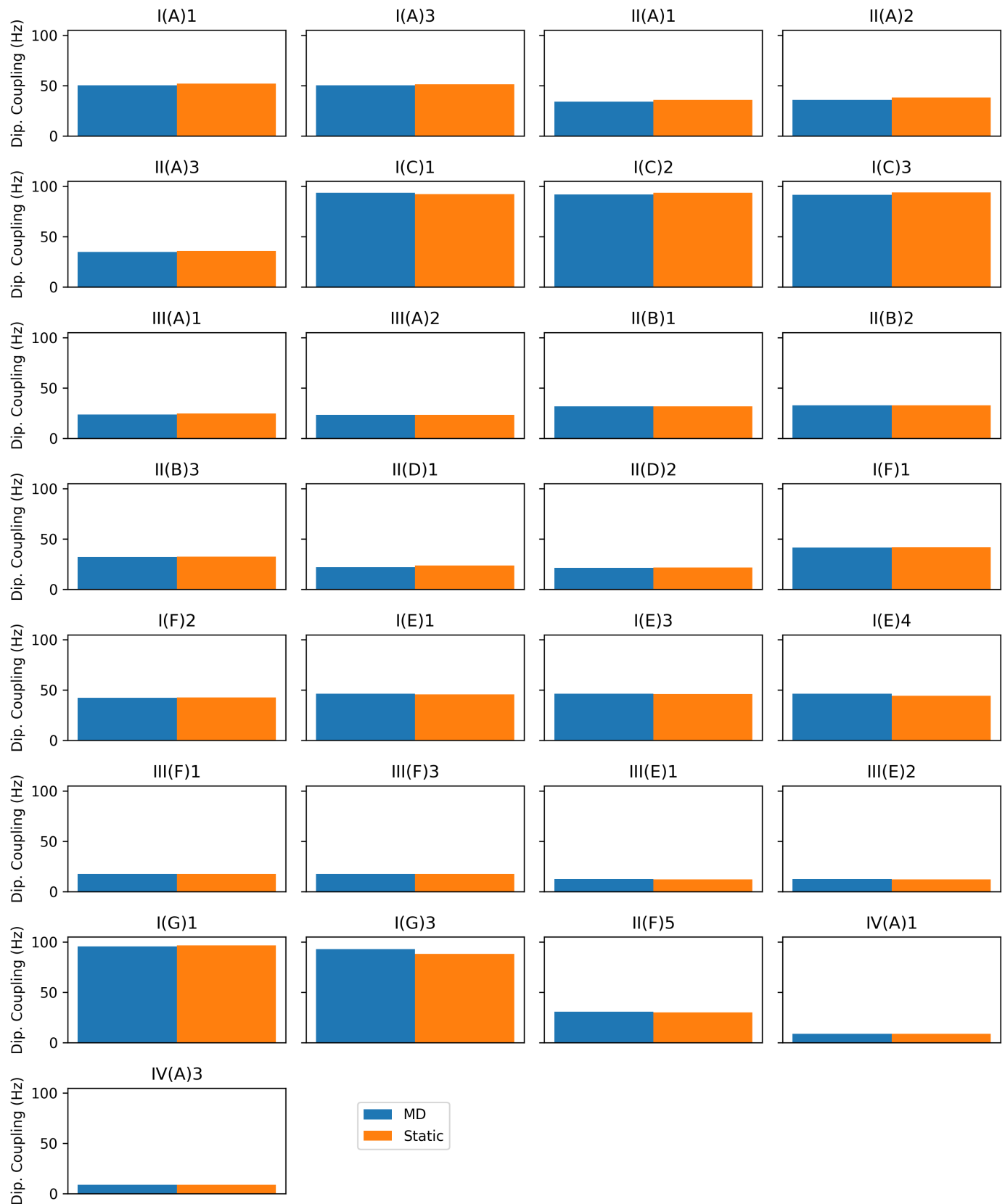


Fig. S15  $^{27}\text{Al}$ - $^{27}\text{Al}$  dipolar couplings calculated from static (blue) and MD trajectory (orange), showing little difference between the two.

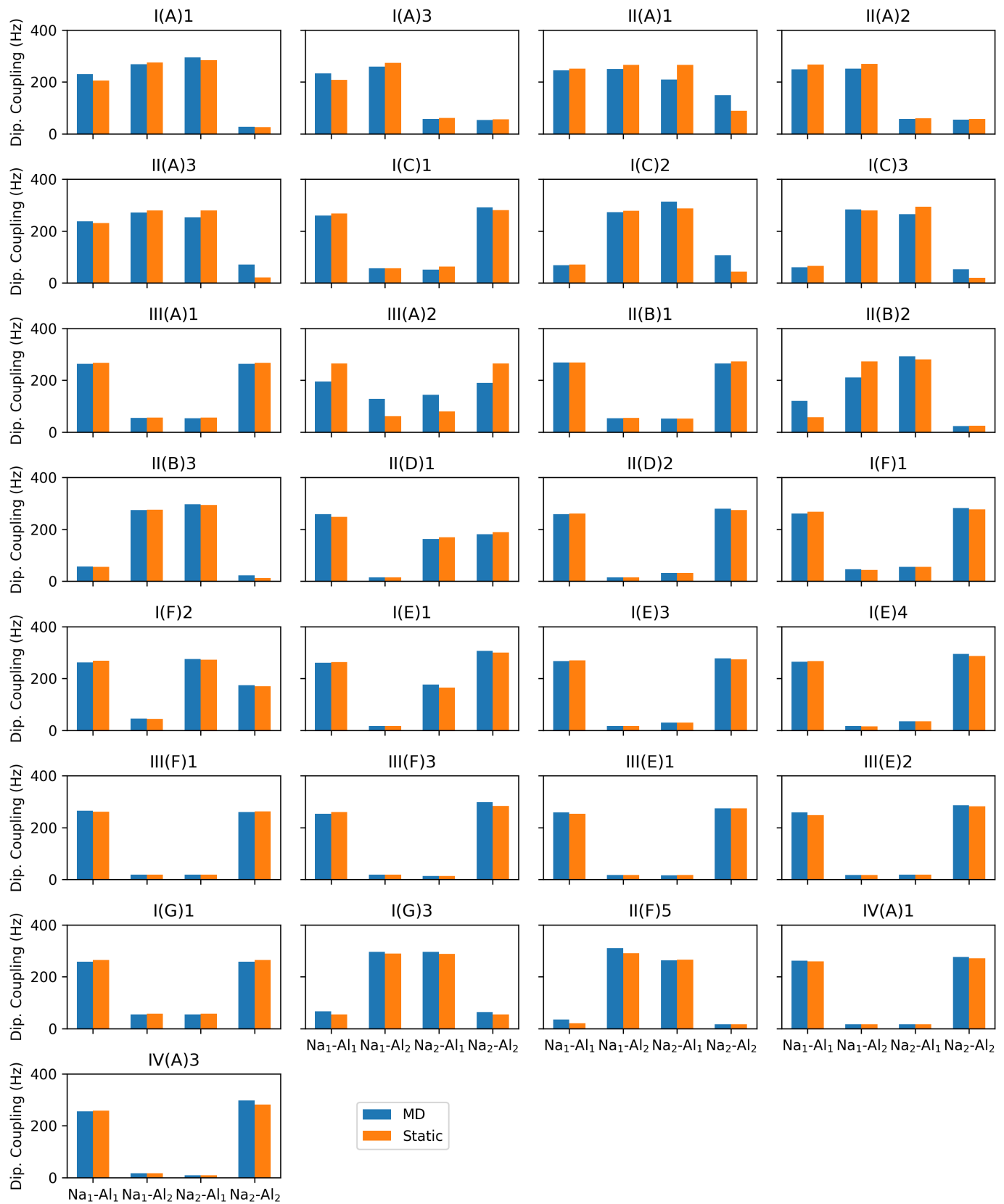


Fig. S16 <sup>23</sup>Na-<sup>27</sup>Al dipolar couplings calculated from static (blue) and MD trajectory (orange).

## 10 Energetic Penalty of 6MR(0Al) configurations

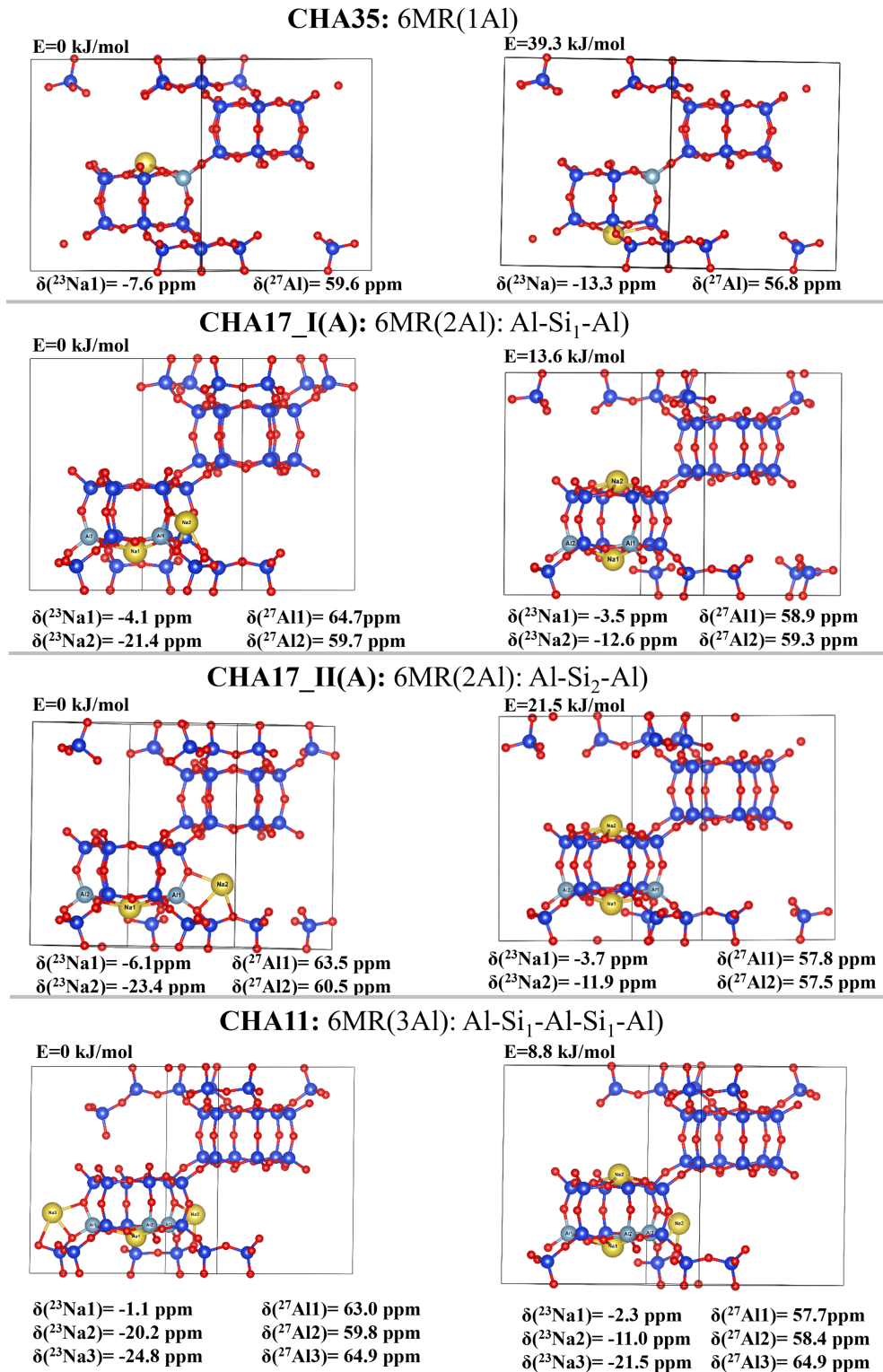


Fig. S17 Structural and energetic comparison of configurations with Na on siliceous six-rings (6MR(0Al)). Left is the global minimum Na arrangement for a given Al distribution, right is the best configuration with a sodium ion in a 6MR(0Al) site. The CHA(35) has only one Al in the d6r unit to form a 6MR(1Al); CHA(17) has two Al to form 6MR(2Al):Al-Si<sub>n</sub>-Al, n=1, 2; and CHA(11) has three to form 6MR(3Al):Al-Si<sub>1</sub>-Al-Si<sub>1</sub>-Al. It is notable that the unusual 6MR(0Al) configuration for Na is increasingly competitive with 6MR(1Al) and 6MR(2Al) configurations as the Si/Al ratio decreases. This configuration has a distinctive Na chemical shift at around -12 ppm, which does not significantly vary with Si/Al ratio.

## 11 Effect of Model and sequence length

In order to isolate the effects of energy cutoff, reference choice, Si/Al ratio and sequence length in the modelling of Na chemical shifts, we compared our protocol to the calculations of Zhao et al.<sup>7</sup> in zeolite CHA. In that work, the authors applied calculations to a cluster model with one and two aluminium sites to reproduce the experimental data for CHA(48), CHA(21) and CHA(4), and thereby assign the positions of the sodium ions. For the isolated Al atom, the 6MR(1Al) configuration, denoted SIIa0 was predicted to be occupied, while for the 2 Al model, the II(A)1 (SIIa1/SIII'a1) configuration was predicted. The authors used 1M NaCl solution as the reference in <sup>23</sup>Na NMR spectra measurement, and solid NaCl is used as a secondary reference (7.1 ppm from the NaCl solution in the calculations, as in ref.<sup>8</sup>).

To fit the DFT static results, the static atomic optimization of periodic models was performed in the Vienna ab initio simulation package (VASP)<sup>9-11</sup> with the general gradient approximation (GGA) Perdew–Burke–Ernzerhof (PBE)<sup>12</sup> functional and included the description of dispersion forces accordingly to the Becke-Johnson (BJ) damping model (PBE+D3)<sup>13</sup>. The wave-function has been converged  $10^{-6}$  eV, the forces reduced below 0.01 eV/Å and the Brillouin zone has been sampled using only Gamma point. Then the NMR calculations were performed in CASTEP with the same set shown in the method session.

We first observe via calculations with periodic models with 2 Al per cell (CHA(17)), that the role of energy cutoff is indeed small, via comparison of 700 and 800 eV cutoff on the chemical shifts for Na atoms (Table S9).

Next, we find that the choice of reference is important, with significant and inconsistent differences between the averaged reference used in this work ( $\delta_1$ ) and the NaCl(s) reference that matches that of Zhao et al. ( $\delta_2$ ). Hence, the choice of reference is likely to play a role in the assignment of chemical shifts to Na locations. Furthermore, we do not obtain a good agreement between calculated  $\delta_2$  shifts at CHA(17) with those calculated by Zhao et al, despite the same referencing method and aluminium content of the models. This highlights the large effect of the model and in particular, the role of Al-Al pairing effects, which differ between cluster and periodic models.

To test the effect of pairing, a  $2 \times 1 \times 1$  supercell was built, with Si/Al = 35, to eliminate the influence from the Al pair in the neighbouring cell. We observe that the <sup>23</sup>Na  $\delta_{iso}$  of the CHA(35) using the NaCl reference reproduces Zhao's calculations closely, and therefore does not agree with the periodic CHA(17) results. This proves that the connection between Al atoms across the cell boundary has a qualitative effect on the environments experienced by the sodium cations, and thus the sequence length is a factor in Na-NMR, as we showed to be the case in recent work on Al-NMR in zeolites CHA and MOR.

As a result of these two significant effects: the referencing method and the Al-pairing lengths, we may re-evaluate the assignment of peaks from the experimental spectra of Zhao et al., focussing on a model which closely matches the experiment. Hence, we compare our CHA(17) model with the experimental CHA(21) data. Using the averaged reference, we find that indeed, the II(A)1 (SIIa1/SIII'a1) configuration may fit the experimental data, with calculated shifts of -6.1/-23.4 matching the experimental values of -7.9/-20.4 fairly well. The large discrepancy between calculation and experiment for SIII'a1 found by Zhao et al. is drastically reduced by the use of a periodic model with the averaged reference. However, there is another configuration in the periodic CHA(17) model which is in reasonable agreement with experimental data. The I(A)1 (SIIa1/SIII'a2) configuration, has peaks at -4.1/-21.4, which may also be assigned to the same experimental signal. Hence, it is not a straightforward task to unambiguously assign the Na locations, and a model which is far from experiment may lead to incorrect predictions.

Finally, we reproduce the "isolated" sodium shift with the CHA(35) (1x1x1) model, obtaining a value of -8.5 ppm. This value agrees well with the experimental shift at CHA(48) of  $-10.5 \pm 2.0$  ppm, while the prediction of -15.99 ppm obtained for the same configuration with the NaCl reference is further from the experimental value.

Table S9 The  $^{23}\text{Na}$  NMR  $\sigma$  and  $\delta$  parameters of CHA(17) and CHA(35).  $\delta_1$  is by using the linear regression formula and  $\delta_2$  is obtained by using NaCl solution as a chemical shift reference. Chemical shifts are quoted in ppm, and energies in  $\text{kJ mol}^{-1}$

Cutoff energy (eV)	800						700						Zhao et.al <sup>7</sup>	
	Al pairs	CHA(17) $1 \times 1 \times 1$			CHA(17) $1 \times 1 \times 1$			CHA(35) $2 \times 1 \times 1$			cluster model $\delta_{\text{calc}}$	CHA(21) $\delta_{\text{exp}}$		
		$\delta_1$	$\delta_2$	E	$\delta_1$	$\delta_2$	E	$\delta_1$	$\delta_2$	E				
SIIa1	-5.5	-13.2	0.0	-6.1	-13.2	0.0	-3.0	-9.6	0.0	-9.3	-7.9			
SIII'a1	-22.6	-33.5		-23.4	-33.5		-18.1	-27.3		-28.8	-20.4			
SIIa1	-1.5	-8.5	27.9	-2.1	-8.5	9.6	0.6	-5.4	8.8	-5.4				
SIII'a1	-21.6	-32.2		-22.4	-32.3		-20.3	-29.8		-28.1				
SIIa2	-3.5	-10.8	0.0	-4.1	-10.9	0.0	-2.2	-8.6	0.0	-11.2				
SIII'a2	-20.6	-31.1		-21.4	-31.1		-17.9	-27.1		-28.9				
SIIa2	-2.2	-9.2	6.7	-2.8	-9.4	0.2	0.6	-5.4	15.9	-7.3				
SIII'a2	-20.9	-31.4		-21.8	-31.5		-18.7	-27.9		-27.8				
Isolated Al	CHA(35) $1 \times 1 \times 1$			CHA(35) $1 \times 1 \times 1$			CHA(71) $2 \times 1 \times 1$							
CHA(35/71) / SIIa0	-7.8	-15.9		-8.5	-16.0		-7.0	-14.23		-11.2	-10.6			

## References

- 1 A. Erlebach, P. Nachtigall and L. Grajciar, *npj Computational Materials*, 2022, **8**, 174.
- 2 S. E. Ashbrook and D. McKay, *Chemical Communications*, 2016, **52**, 7186–204.
- 3 T. Charpentier, S. Ispas, M. Profeta, F. Mauri and C. J. Pickard, *The Journal of Physical Chemistry B*, 2004, **108**, 4147–4161.
- 4 H. Koller, G. Engelhardt, A. P. M. Kentgens and J. Sauer, *The Journal of Physical Chemistry*, 1994, **98**, 1544–1551.
- 5 J. Steinadler, O. E. O. Zeman and T. Bräuniger, *Oxygen*, 2022, **2**, 327–336.
- 6 C. Lei, A. Erlebach, F. Brivio, L. Grajciar, Z. Tošner, C. J. Heard and P. Nachtigall, *Chemical Science*, 2023, **14**, 9101–9113.
- 7 Z. Zhao, Y. Xing, S. Li, X. Meng, F.-s. Xiao, R. McGuire, A.-N. Parvulescu, U. Müller and W. Zhang, *The Journal of Physical Chemistry C*, 2018, **122**, 9973–9979.
- 8 R. K. Harris and G. J. Nesbitt, *Journal of Magnetic Resonance (1969)*, 1988, **78**, 245–256.
- 9 G. Kresse and J. Hafner, *Physical Review B*, 1994, **49**, 14251–14269.
- 10 G. Kresse and J. Furthmüller, *Computational Materials Science*, 1996, **6**, 15–50.
- 11 T. Charpentier, *Solid State Nuclear Magnetic Resonance*, 2011, **40**, 1–20.
- 12 J. P. Perdew, K. Burke and M. Ernzerhof, *Physical Review Letters*, 1996, **77**, 3865–3868.
- 13 S. Grimme, S. Ehrlich and L. Goerigk, *Journal of Computational Chemistry*, 2011, **32**, 1456–1465.